



HAL
open science

Site-and species-specific bacterial communities in two crustose coralline algae from the NW Mediterranean Sea

Elisabetta Manea, Lorenzo Bramanti, Laura Pezzolesi, Annalisa Falace, Sara Kaleb, Lucia Bongiorni, Pierre E. Galand

► To cite this version:

Elisabetta Manea, Lorenzo Bramanti, Laura Pezzolesi, Annalisa Falace, Sara Kaleb, et al.. Site-and species-specific bacterial communities in two crustose coralline algae from the NW Mediterranean Sea. 2024. hal-04441255

HAL Id: hal-04441255

<https://hal.science/hal-04441255>

Preprint submitted on 6 Feb 2024

HAL is a multi-disciplinary open access archive for the deposit and dissemination of scientific research documents, whether they are published or not. The documents may come from teaching and research institutions in France or abroad, or from public or private research centers.

L'archive ouverte pluridisciplinaire **HAL**, est destinée au dépôt et à la diffusion de documents scientifiques de niveau recherche, publiés ou non, émanant des établissements d'enseignement et de recherche français ou étrangers, des laboratoires publics ou privés.



Distributed under a Creative Commons Attribution 4.0 International License

Site- and species-specific bacterial communities in two crustose coralline algae from the NW Mediterranean Sea

Manea, E.^{1*}, Bramanti, L.¹, Pezzolesi^{2,3}, L., Falace, A.⁴, Kaleb, S.⁴, Bongiorni, L.⁵, Galand, P.E.¹

¹Laboratoire d'Ecogéochimie des Environnements Benthiques, LECOB, Observatoire Océanologique de Banyuls sur Mer Centre National de la Recherche Scientifique (CNRS)-Sorbonne Université, Banyuls sur Mer, France

²Department of Biological, Geological and Environmental Sciences (BiGeA), University of Bologna, Via Sant'Alberto 163, 48123 Ravenna, Italy

³Interdepartmental Centre for Industrial Research in Renewable Resources, Environment, Sea and Energy (CIRI-FRAME), University of Bologna, Via Sant'Alberto 163, 48123 Ravenna, Italy

⁴Department of Life Sciences, University of Trieste, Via Licio Giorgieri 10, 34127 Trieste, Italy

⁵Institute of Marine Sciences, National Research Council, CNR-ISMAR, Arsenale, Tesa 104, Castello 2737/F, 30122, Venice, Italy

*Corresponding author: elisabetta.manea@obs-banyuls.fr

Highlights

- *Lithophyllum stictiforme* and *Mesophyllum* sp. as reservoirs for bacterial diversity
- The two CCA morphotypes host distinct bacterial communities
- Neighboring CCA thalli of the same morphotype host more similar bacteria communities
- All the studied CCAs host bacteria potentially involved in coral larvae settlement

Abstract

Crustose coralline algae (CCAs) are one of the main components of coralligenous, one of the most diverse marine habitats in the Mediterranean Sea. Beyond their role as ecosystem engineers,

certain CCAs have been shown to favor the settlement of gorgonian larvae, an important capacity in the context of the restoration of these species. Similarly to other species, CCAs live associated to symbiotic microorganism forming a holobiont. Despite their ecological importance and vulnerability to climate change, Mediterranean CCA holobionts have been understudied in terms of taxonomy and microbiome. Using electron microscopy and barcoding techniques, we identified *Lithophyllum stictiforme* complex and the genus *Mesophyllum*, two widespread CCA morphotypes from the Western Mediterranean Sea, which are often found in close proximity with gorgonians. 16S rRNA amplicon sequencing revealed that these two CCAs harbor distinct and diverse bacterial communities. Bacterial communities also differ between thalli of the same CCA morphotype, showing greater similarity between neighbor thalli, suggesting that exogenous factors acting at small spatial scale may influence bacterial composition. The predominance of bacterial sequences affiliated to the *Blastopirellula* genus and *Pir4_lineage* of the phylum Planctomycetes in all CCA individuals examined is noteworthy. These bacterial groups have been hypothesized to promote tropical coral larvae settlement, raising the possibility of a similar positive interaction between CCAs and Mediterranean coral larvae.

Keywords: marine holobiont, microbiome, *Lithophyllum stictiforme*, *Mesophyllum*, gorgonians, marine monitoring

1. Introduction

Crustose coralline algae (CCAs) are characteristic of Mediterranean coastal and mesophotic seascape (Ballesteros, 2006; Castellan et al., 2019; Bracchi et al., 2022). They are key components

of coralligenous concretions, which, with their large spatial and bathymetric extent (up to 2,700 km² in surface and from 20 to 130 m depth; Martin et al., 2014, Iborra et al., 2022), are among the most representative and biodiverse Mediterranean benthic habitats. CCAs are recognized as the group of rhodophytes potentially hosting the greatest cryptic diversity at both species and genus level, and Mediterranean CCAs are no exception (Pezzolesi et al., 2019; Rindi et al., 2019). Due to their calcareous and three-dimensional thalli, CCAs play a key role as ecosystem engineers, thus supporting a high biodiversity (Asnaghi et al., 2015; Pezzolesi et al., 2017; Piazzini et al., 2022). Despite vulnerability to temperature anomalies and ocean acidification has been observed mainly in tropical CCA species, Mediterranean CCAs have also been impacted by the effect of climate change, as well as by pathogenic diseases (Martin & Gattuso, 2009; Short et al., 2015; Quéré et al., 2019; Cornwall et al., 2022; Vitelletti et al., 2023). Events of spread CCA mortality have been recorded in the Mediterranean Sea (Hereu & Kersting, 2016), and thus, studies focusing on these algae are needed to better assess coralligenous biodiversity and health state.

The taxonomy, biology, and distribution of CCAs have only been studied for a small number of Mediterranean species, and sometimes the information on their diversity is still limited and not exhaustive. One of the least explored areas of research into Mediterranean CCAs is their associated microbiome (Rindi et al., 2019). To date, only two studies have addressed this topic focusing on a single species, *Neogoniolithon brassica-florida* (Quéré et al., 2019; Gefen-Treves et al., 2021). These studies provided first insights into CCA-bacteria associations and emphasized the need to better understand the functioning of these holobionts. Indeed, there is evidence of species-specific CCA microbiomes (Barott et al., 2011; Cavalcanti et al., 2014; Sneed et al., 2015) and hosted bacteria that can be key players in algae morphological development, possessing also antifouling properties against epibionts (Singh & Reddy, 2016; Gómez-Lemos & Guillermo Diaz-

Pulido, 2017; Singh et al., 2017). The microbial community could also be an indicator of the health status of the algae and the habitats they colonize (Glasl et al., 2017; Quéré et al., 2019). Further studies on Mediterranean CCAs are needed to provide the basis for future monitoring studies.

It has been shown that CCAs are involved in the recruitment processes of several invertebrate species (Lau et al., 2005; O’Leary et al., 2017; Seabra et al., 2019), promoting, for instance, the settlement and metamorphosis of tropical coral larvae (Gómez-Lemos et al., 2018; Siboni et al., 2020; Jorissen et al., 2021). In the Mediterranean Sea, field observations and an experimental study also showed gorgonian-CCA interactions (Toma et al., 2022; Zelli et al 2020). Gorgonians are priority species for conservation and are among those most threatened by climate change and local impacts (Iborra et al., 2022; Tignat-Perrier et al., 2022; Chatzimentor et al., 2023). In recent decades, in particular, mass mortality events related to effects of marine heat waves have led some shallow Mediterranean gorgonians populations at risk of collapse (10-30 m, Garrabou et al., 2022; Bramanti et al., 2023). Initiatives are underway to conserve and even reintroduce these species to their natural habitat (e.g., Bramanti et al., 2007; Linares et al., 2008; Montseny et al., 2019; Casoli et al., 2022). In this context, knowledge on CCA holobionts could provide new information for restoration strategies.

In this study, we analyzed the diversity of the bacteria associated with two widespread CCAs in the Western Mediterranean Sea that are colonized by or located near gorgonians. We identified the taxonomy of the CCA species based on their morphological traits and molecular techniques. Through DNA metabarcoding, we deciphered the diversity of CCA bacteria at the lowest possible taxonomic level to assess species-specific CCA bacteria associations. Then, we explored the sharing and uniqueness of bacteria diversity both among individuals belonging to the same CCA taxonomic group, as well as among individuals belonging to the two different CCAs.

2. Material and Methods

2.1 Samples collection and preparation

Thalli of two of the most widespread morphotypes of CCA (ca. 5 cm wide and 5-10 cm long) were collected in December 2022 at the Canadels site in Banyuls-sur-Mer, France (42°26.900' N, 3°10.347' E). The sampling area harbors populations of two octocoral species: the white gorgonian (*Eunicella singularis*) and the red coral (*Corallium rubrum*). The collection focused on subtidal CCA species with a coarse morphology corresponding to the *Lithophyllum stictiforme* complex, namely morphotype 1 (see Pezolesi et al., 2019), and *Mesophyllum* spp., namely morphotype 2 (see Peña et al., 2015). Morphotype 1 specimens formed crusts, blades, or lamellae of varying thickness, not strongly adherent to the substrate and with smooth surface; while morphotype 2 specimens were encrusting, occasionally unattached, usually with surface protuberances. The morphotypes were sampled in three distinct and adjacent sampling sites (morphotype 1: ST25, ST27, ST7; morphotype 2: ST12, ST13, ST17), in three replicates (i.e., three distinct thalli from each site), for a total of 18 samples. Samples were collected using hammer and chisel at 25 m depth within an area of approximately 30 m² by SCUBA diving. Considering the high crypticity of CCA species (Rindi et al., 2019), which often leads to a scant reliability of morphological traits for species identification, the sampling was restricted to a small geographical area with the intention of collecting thalli of the same species.

In the laboratory, the epiphytes were carefully removed from the CCA surface. After cleaning, each CCA thallus was divided into fragments, half of which were collected with sterile forceps and immediately frozen at -80°C for subsequent bacteria DNA extraction. The other half of the fragments were air-dried and stored in plastic bags with silica gel until CCA morpho-

anatomical characterization and DNA extraction. A volume of 2 L of seawater was also collected at the sampling sites by using sterile bags, for a total of 9 water samples, for analysis of seawater bacteria diversity to be used as a control. Water samples were immediately prefiltered through a 0.7 µm filter (Glass microfiber filters GF/F, 47 mm filtered, Whatman) and subsequently through a 0.2 µm filter (Nuclepore Track-Etch Membrane, diameter 47 mm, Whatman). The filters were frozen at -80°C until bacteria DNA extraction.

2.2 Morpho-anatomical characterization of CCA

For detailed description of morpho-anatomy, all CCA individuals were examined with a scanning electron microscope (SEM) according to Kaleb et al. (2018). Small fragments of the thalli were mounted on aluminum stubs with acrylic adhesive, and then coated with a thin layer of chromium (Quorum Q150T ES coater) and analyzed with a SEM Zeiss Gemini300 at a working distance (WD) between 8 and 11 mm.

2.3 CCA DNA extraction, amplification and sequencing

The silica-dried CCA samples were pulverized using sterile mortars and the DNA extraction was performed following the modified protocol of the Qiagen DNeasy Blood & Tissue Kit (Qiagen, Crawley, UK) by Broom et al. (2008). The *psbA* gene was PCR-amplified in both morphotypes according to Pezzolesi et al. (2017, 2019), while the mitochondrial COI-5P fragment was PCR-amplified in morphotype 2, to increase the number of reference sequences available for the subsequent alignment, following Peña et al. (2015). PCR products were visualized in 1.5% agarose gels stained with Midori Green using Low DNA Mass Ladder (Invitrogen, Carlsbad, CA, USA)

as a reference, and PCR products with expected lengths and yields were purified and sequenced by BMR Genomics (Padua, Italy).

2.4 CCA sequence alignments and phylogenetic analyses

The quality of the sequences was assessed by visual inspection of the electropherograms using the Chromas software (Version 2.6.6; Technelysium Pty LTD, South Brisbane, Australia). All sequences were found to be of high quality, without double or confounding peaks, and were all retained for the alignment and phylogenetic analyses. Alignment was performed using ClustalW and default settings in AliView software (Version 1.28; Larsson, 2014) and phylogeny constructed by means of MEGA software (Version 11.0.13, www.megasoftware.net; Tamura et al., 2021). In addition, NCBI database (www.ncbi.nlm.nih.gov) was searched for publicly available sequences of *Lithophyllum stictiforme* complex and *Mesophyllum* genus, and some representatives were selected to be included in the alignments. The alignment was assembled after a series of preliminary phylogenetic analyses aimed at correct selection of ingroup and outgroup taxa. Therefore, *psbA* sequences of *Lithophyllum dentatum* (Kützing) Foslie, *L. hibernicum* Foslie, and *L. bathyporum* Athanasiadis & D.L.Ballantine, and *psbA* and COI-5P sequences of the Melobesioideae *Phymatolithon calcareum* (Pallas) W.H. Adey & McKibbin and *Lithothamnion corallioides* (P.L. Crouan & H.M. Crouan) P.L. Crouan & H.M. Crouan were included as outgroups in the respective data sets, according to previous studies (Pezzolesi et al, 2019; Peña et al., 2015). The sequences' alignment of *L. stictiforme* *psbA* sequences was 825 bp long, while those of *Mesophyllum* ranged from 598 (S17R1), 684 (S17R2), 725 (S12R1) to 851 base pairs (bp). The COI-5P of *Mesophyllum* alignment resulted in 608 bp. Neighbor-Joining (NJ) distance analyses were performed on all data sets using Maximum Composite Likelihood model in MEGA

software, with nodal support assessed by 1,000 bootstrap (BR) resamplings. Phylogenetic relationships were inferred using Maximum likelihood (ML) analyses in MEGA software, under a generalized time-reversible with gamma+invariant sites heterogeneity model (GTR+G+I), and a generalized time-reversible gamma distributed (GTR+G) alignments, for the COI-5P and psbA alignments respectively. The bootstrap consisted of 1000 replicates with complete deletion option, i.e. eliminating the positions containing gaps and missing data (Saitou & Nei, 1987; Nei & Kumar, 2000; Pezzolesi et al., 2019).

2.5 Bacteria DNA extraction and sequencing

Frozen CCA samples were pulverized using sterile mortars. Total genomic DNA was extracted from 18 CCA samples and 9 seawater samples using Power Soil DNA Isolation kit and Power Water DNA Isolation kit, respectively, according to the manufacturer's instructions (QIAGEN, Hilden, Germany). After DNA quantification, analyses of the prokaryotic 16S rDNA sequences were conducted through amplicons generation with the use of primers amplifying the bacterial V3-V4 region (Klindworth et al., 2013), and sequencing was performed on the Illumina MiSeq V3 platform at the Integrated Microbiome Resource (IMR, imr.bio, Dalhousie University, Halifax, Nova Scotia, Canada) to obtain 2x300 paired-end sequences.

2.6 Bacteria sequence analyses

The sequences were processed with the DADA2 package, version 1.16 (Callahan et al., 2016) in R 4.2.3 (R Core Team, 2023). After inspection of quality control profiles, the filtering parameters were set as follow: truncLen=c(280,220), trimLeft=c(17,21), maxN=0, maxEE=c(2,5), truncQ=2, rm.phix=TRUE, compress=TRUE, multithread=TRUE. The sequences were then dereplicated,

denoised by removing sample inference and chimeras, and merged. Representative amplicon sequence variants (ASVs) were classified against the SILVA version 138.1 database (McLaren & Callahan, 2021). The dataset was cleaned from chloroplast, Archaea, unknown ASVs at the phylum level and singletons with the R package phyloseq (McMurdie & Holmes, 2013). After cleaning, a total of 503,450 reads and 2599 ASVs were retained.

Rarefaction curves were produced by rarefying the dataset to 9310 sequences through the use of vegan package in R (Oksanen et al., 2013). To estimate CCA-bacteria communities alpha-diversity, the phyloseq package was used to calculate the Shannon Index with the *diversity* function. Significant differences among alpha-diversity values of sampling sites were tested. The Shapiro Wilk test was applied to test for normality of data. Because data were non-normal, the Kruskal-Wallis test followed by the Dunn test (dunn.test package) were used. A multidimensional scaling ordination (MDS), based on Bray-Curtis distance matrix computed from Hellinger transformed data, was constructed with the vegan package to visualize similarities in bacteria community composition both between CCA morphotypes and within samples of the same CCA morphotype. A permutational multivariate analysis of variance (PERMANOVA) was used to test for significant differences among bacteria communities associated with thalli of the same CCA morphotype. The analysis was performed on ASVs relative abundance (as percentage contribution of sequences of one ASV to the total number of sequences) on Bray Curtis distance matrix of Hellinger transformed data considering the sampling sites as source of variance and using 999 permutations under reduced model. The PERMANOVA was also applied to assess the diversity among CCA morphotypes and water bacteria communities.

ASVs shared between all CCA-bacteria communities and water samples and between individual CCA-bacteria communities within CCA morphotypes were identified using the

microbiome package (Lahti et al., 2017) and the *core_members* function (Salonen et al., 2012). Among both the shared and unique ASVs associated to the two CCA morphotypes and characteristic of each morphotype, the five most abundant ASVs were selected for further taxonomic analysis through a manual BLAST search against the NCBI nucleotide library (<https://blast.ncbi.nlm.nih.gov/Blast.cgi>).

3. Results

3.1 CCA morpho-anatomy

According to morpho-anatomical analyses, all individuals of morphotype 1 belong to *Lythophyllum stictiforme* complex and no substantial differences in diacritical features were found between the individuals from the three sampling sites, except for a different number of epithallial cells. The thalli were encrusting with a free laminar margin and the surface was flat or undulating (Fig. 1A, Suppl. Fig. 1A). The thallus construction was dimerous (Fig. 1B, Suppl. Fig. 1B), with a monostromatic ventral region. In all individuals, the epithallus was abraded (Fig. 1C, Suppl. Fig. 1C), sometimes exposing the underlying cell layer. The filaments of the thallus end at the surface with 1-2 epithallial cells with a flat or slightly convex distal cell wall (Fig. 1D). In the individuals collected at site ST25, filaments with 2-3 epithallial cells (Suppl. Fig 1D) occurred in patches and were interspersed with patches of filaments with one epithallial cell. Epithallial cells were subtended by square or rectangular meristematic cells (Fig. 1D). The cells of the ventral region were square (non-palisade), giving rise to the peripheral filaments which consisted of square or rectangular cells, connected laterally by secondary pit connections (Fig. 1E). The thalli bore uniporate conceptacles that protruded slightly in surface view (Fig. 1F, Suppl. Fig. 1E), or were

sometimes flush with the surrounding thallus surface. All individuals were tetrasporangial. The conceptacles were dumbbell-shaped with a prominent central columella and the laterally arranged tetrasporangia (Figs. 1B, G, H, Suppl. Fig. 1F).

Individuals of morphotype 2 were encrusting to warty (Fig. 2A) and exhibited the features considered diagnostic for the genus *Mesophyllum* Lemoine. The combination of morpho-anatomical features differed from previously described species, so we identified them as *Mesophyllum* sp. In surface view, large areas of shedding epithallial cells were observed in all thalli (Fig. 2B) and the epithallial cells were flared (Fig. 2B, C). Thalli were dorsiventrally organized and had monomerous construction with the core region exhibiting a coaxial growth (i.e., cells of adjacent filaments in core region aligned in arching tiers) (Fig 2D, E). Cells of adjacent filaments were connected by fusions. The individuals bore scattered or densely grouped multiporate conceptacles protruding above the surrounding thallus surface (Fig. 2A, D). Mature conceptacles had a peripheral rim and a slightly sunken central pore plate (Fig. 2D, F). Conceptacle chamber floors were 10-12 cells deep in the peripheral region and had no contact with the core region (Fig. 2D). In surface view, the pore canals were bordered by 8-10 cells that were smaller than the adjacent epithallial cells (Fig. 2G). In section, the cells lining the basal and median part of the pore canal were square and larger than the other cells forming the conceptacle roof, while in the upper part of the pore the lining cells were flattened (Fig. 2H). In individuals R2 collected at ST12 and R3 collected at ST13, only immature conceptacles were observed, so it was not possible to assign them to the main group of samples due to lack of relevant features.

3.2 CCA phylogeny

For morphotype 1, the molecular phylogeny analysis based on the *psbA* marker confirmed that all 9 individuals belonged to the *Lithophyllum stictiforme* complex, previously described as formed by numerous clades (Pezzolesi et al., 2019). Clade 3B included 6 samples from this study belonging to two of the three collection sites, together with some reference sequences from Italy and two from France, including also one (isolate LLG3464) from the sampling area of the present study (S27 and S7; Fig. 3). Replicates collected at site S25 all fell within a distinct haplogroup defined as C3 (de Jode et al., 2019). It contained closely similar reference sequences (99% similarity) from samples previously collected from the same study area (i.e., Banyuls sur Mer).

For morphotype 2, 8 out of the 9 *psbA* sequences generated in this study clustered with a Mediterranean *M. macroblastum* specimen (voucher VPF00506), collected in the Alboran Sea (Spain), and with the Uncultured Corallinales clone LBC0055, collected close to the study area (42.497219 N, 3.135617 E; Bittner et al., 2010; Fig. 4). The last sequence (S12R2) was closely related to the main cluster. For the COI-5P marker, only 5 sequences were generated as all amplification attempts for station 13 samples were unsuccessful. The phylogenetic tree obtained from the ML analysis of the COI-5P alignment was congruent with the *psbA* tree (Fig. 5). It grouped our sequences within a big clade of Mediterranean *M. macroblastum* with high support (99%), well separated from the other *Mesophyllum* species (*M. alternans*, *M. expansum*, *M. lichenoides*, *M. erubescens*, and *M. sphaericum*) (Fig. 5). Our samples were more closely associated to three haplotypes, specifically to haplotype 1 (KJ592663), 4 (KJ592666) and 5 (KJ592637 and KJ592694), as previously reported by Peña et al. (2015).

3.3 Bacterial community diversity

Rarefaction curves based on 16S rRNA ASVs reached a plateau for all samples indicating that the CCA associated bacteria diversity was well covered (Suppl. Fig. 2).

The average Shannon values ranged between 4.7 ± 0.1 and 5.5 ± 0.2 , and between 5.7 ± 0.3 and 6 ± 0.1 in *L. stictiforme* and *Mesophyllum* sp. samples, respectively (Fig. 6A). No significant differences in diversity were found among individuals of the same morphotype. The lowest values were recorded for *L. stictiforme* taken at site ST27. In *Mesophyllum* sp. sampling sites ST13 and ST17 values were significantly higher than in ST27 (one of *L. stictiforme* sampling site, p -value $< 0.05^*$). In ST17 the value was also significantly higher than in *L. stictiforme* sampling site ST25 (p -value $< 0.05^*$, Fig. 6A). The observed ASV numbers varied between 302 and 898 in the low diversity site ST25 (*L. stictiforme*; on average 335-600 ASVs among sampling sites), and one sample at site ST13 (*Mesophyllum* sp.; on average 626-740 ASVs among sampling sites), respectively (Fig. 6B).

In the MDS ordination of microbial community composition, samples of *L. stictiforme* clustered separately from the ones belonging to *Mesophyllum* sp. (Fig. 7). Among *L. stictiforme* samples, those from ST27 and ST7 were closer to each other than those from ST25. *Mesophyllum* sp. samples from sites ST12 and ST17 clustered together more tightly than those collected in site ST13.

The comparison of bacteria communities associated to the same CCA morphotype showed significant differences (p -value = 0.005^{**} , *L. stictiforme* bacteria communities; p -value = 0.002^{**} , *Mesophyllum* sp. bacteria communities). Finally, the bacterial community composition of the water was significantly different from those of the CCAs (p -value = 0.001^{***}).

3.4 CCA bacterial community composition

The taxonomy of CCA-associated bacteria was first analyzed at the class and order levels considering the five most contributing taxa as relative abundance across the dataset. At the class level, the bacterial communities of both CCA morphotypes were dominated by Alphaproteobacteria, which accounted for 40% and 46% of the sequences in *L. stictiforme* and *Mesophyllum* sp., respectively (Supp. Fig. 3A, C). They were followed by Gammaproteobacteria (18% and 10%), Acidimicrobiia (12% and 5%), Planctomycetacia (9% and 18%) and Bacteroidia (5% and 7%). At the order level, the most abundant group in *L. stictiforme* was *Rhizobiales* (15%), while in *Mesophyllum* sp. it was *Pirellulales* (18%) (Supp. Fig. 3B, D). These two orders were shared by the two CCAs. The order *Rhodobacterales* was also shared, while *Cellvibrionales* and *Microtrichales* (8% and 12%), and *Flavobacteriales* and *Rhodovibrionales* (6% and 7%) were abundant only in *L. stictiforme* and *Mesophyllum* sp. bacteria communities, respectively.

At the family level, among the 20 most contributing families, *Pirellulaceae* (phylum Planctomycetes) were present and abundant in all CCA bacteria assemblages, contributing on average 4.5-15% to *L. stictiforme* bacteria communities in ST25 and ST7, and 13-23.4% to *Mesophyllum* sp. bacteria communities in ST13 and ST12, respectively (Fig. 8A, B). Shared bacteria families were also *Microtrichaceae* (phylum Actinobacteria) and *Rhodobacteraceae* (class Alphaproteobacteria), more abundant in *L. stictiforme* (average percentage contribution 7.4-15% in ST7 and ST25 samples, and 5.8-11.4% in ST25 and ST7 samples, respectively), and *Kiloniellaceae* (class Alphaproteobacteria) and *Flavobacteriaceae* (class Bacteroida) more abundant in *Mesophyllum* sp., with average contribution of 3.1-12.5% in ST12 and ST13 and 4.1-6.9% in ST13, respectively.

Despite these similarities, at the family level there were both inter- and intra-CCA morphotype differences. *Spongiibacteraceae* (class Gammaproteobacteria) and *Stappiaceae*

(class Alphaproteobacteria) were mainly found in *L. stictiforme*, and within this morphotype these bacteria were only abundant in ST27 and in ST25, respectively, with a respective average contribution of 23.2% and 6.8% (Fig. 8A).

At the genus level, among the 10 most contributing genera only three were shared between the two CCA morphotypes: *Geminicoccaceae* NA, *Pir4_lineage* and *Blastopirellula* (Fig. 9). All the other genera were uniquely associated with one of the two CCAs. In particular, *Microtrichaceae* NA (phylum Actinobacteria) and BD1-7_clade were abundant in *L. stictiforme*, while an unknown genus belonging to Alphaproteobacteriaceae and *Bythopirellula* highly contributed to *Mesophyllum* sp. microbiome (Fig. 9).

3.5 Core and unique bacteria

No bacterial ASVs were found to be shared between water and CCAs, while 65 ASVs (2.5%) were shared between *L. stictiforme* and *Mesophyllum* sp. (Fig. 10A). A total of 86 (3.3%) and 154 (5.9%) ASVs were unique to *L. stictiforme* and *Mesophyllum* sp., respectively. When comparing sampling sites, in *L. stictiforme*, 23 ASVs (0.5% of the total ASVs of *L. stictiforme* bacteria) were present at all sites, with sites ST7 and ST27 sharing the highest number of ASVs (20) (Fig. 10B), while between individuals collected in the same site, 4.2 to 7.5% of ASVs were shared among samples of ST27 and among samples of ST25, respectively (Figs. 10B, D). In *Mesophyllum* sp., 84 ASVs (1.4% of the total *Mesophyllum* sp. bacteria ASVs) were found in all sites, and ST12 and ST17 shared the most ASVs (40) (Fig. 10B), while for *Mesophyllum* sp. samples collected in the same site, the percentage of shared ASVs ranged between 11.3-15.4% among samples of ST12 and ST13, respectively (Figs. 10C, E).

Among the shared ASVs, ASVs 13 and 24 belonged to *Filomicrobium* species, ASV 39 was identified as *Ruegeria atlantica*, ASV 48 to *Sva0996_marine_group*, and ASV 14 belonged to the family *Rhizobiaceae* (Table 1). Among the ASVs uniquely associated to and shared only within each CCA morphotype's bacterial communities, ASVs of the genera *Pir4_lineage* and *Blastopirellula* were present in all CCA bacteria assemblages.

4. Discussion

Our study shows that CCA individuals belonging to diverse haplotypes of both *Lithophyllum stictiforme* and *Mesophyllum* sp. morphotypes can be found within a restricted sampling area with homogenous landscape. The morpho-anatomical identification of morphotype 1 confirmed its identity as *L. stictiforme*. Molecular taxonomy results also revealed that two out of the three sampling sites hosted individuals of clade 3B, while the CCAs collected in ST25 belonged to C3 haplotype. This latter has been previously and uniquely identified in the same sampling area (Pezzolesi et al., 2019; de Jode et al., 2019). Further studies are needed to assess a possible endemism of this haplotype in the Banyuls area. As for morphotype 2, despite the presence of the diagnostic characters of *Mesophyllum* genus, their combination differed from the previously described *Mesophyllum* species. Indeed, while the phylogenetic tree clustered some of our samples with different haplotypes of Mediterranean *Mesophyllum macroblastum*, the morphological analysis revealed that the individuals differed from this species in several diacritic features (see Kaleb et al. 2011; Peña et al 2015). Our results highlight the need to further investigate *M. macroblastum* taxonomic and/or nomenclatural status (Guiry & Guiry, 2023). Pending further studies, we nevertheless identified CCA morphotype 2 as *Mesophyllum* sp.

Moving to the bacteria communities, rarefaction analysis showed that we were able to cover the whole bacteria diversity associated with both CCAs. All the analyzed bacteria assemblages presented similar or even higher diversity compared to CCA microbiomes from other marine regions (see for instance Barott et al., 2011; Hester et al., 2016 and Yang et al., 2021). Mediterranean CCAs can thus represent bacteria diversity reservoirs, and further research on these holobionts could help assessing the Mediterranean microbial biodiversity and understanding their role in coralligenous habitat functioning.

Bacterial communities of the two CC taxa were different, with those of *Mesophyllum* sp. showing higher diversity. Studies from other geographic areas have also described species-specific microbiomes for other CCA species (e.g., see Barrott et al., 2011 - Caribbean; Sneed et al., 2015 - Belize; Brodie et al. 2016 - UK). Interestingly, in our study, we also showed distinct bacterial communities among CCAs of the same morphotype, even though they were collected in a very restricted area. Bacterial communities of macroalgae taxa, including CCAs, have been showed to be variable among individuals of the same species (Staufenberger et al. 2008; Burke et al. 2011; Barott et al. 2011; Miranda et al. 2013; Gefen-Treves et al., 2021). Previous studies linked this variability to a difference in environmental conditions determined by geographic distance, depth gradient, seasonality, and exogenous factors, such as anthropogenic influences (Gefen-Treves et al., 2021). These factors can hardly explain our results since CCA thalli were collected simultaneously and in a narrow area. Nevertheless, it is possible that variations in micro-environmental conditions, both above and within CCA tissues (see for instance Valdespino-Castillo et al., 2021), along with selective predatory pressure acting on individual CCA thalli determined the observed differences between individuals of the same morphotype. Other explaining factors could be the variability in the exfoliation mechanism of the superficial cell layer

in CCAs, which may differently affect bacteria colonization and exert selectivity on bacteria taxa limiting the development of mature bacteria communities, and the life stage of the algae, which may influence the diversity of the microbiome that may increase with age (Bengtsson et al., 2012; Sneed et al., 2015).

In both CCAs, at the class level, all the bacteria communities were dominated by Proteobacteria, especially Alpha and Gammaproteobacteria, followed by Planctomycetacia, Acidimicrobia and Bacteroidia. These dominant groups have been found in most of the CCAs investigated in past studies (Barott et al., 2011; Sneed et al., 2015; Brodie et al., 2016; Cavalcanti et al., 2018; Gefen-Treves et al., 2021). At the order level we also identified bacteria taxa already found associated with CCAs, mainly *Rhodobacterales*, *Rhizobiales* and *Rhodovibrionales*, all Alphaproteobacteria (Cavalcanti et al., 2014; Hester et al., 2016; Quéré et al., 2019). These results show that the Mediterranean CCAs host bacterial communities similar to those of other CCAs worldwide at least at the class and order levels.

The dominant families were also the most shared among CCAs, even though in different proportions. *Microtrichaceae* and *Rhodobacteriaceae*, which were abundant in *L. stictiforme* individuals, were also among the most representative families in *Mesophyllum* sp., while *Kiloniellaceae* and *Flavobacteriaceae*, predominant in *Mesophyllum* sp., were also abundant in *L. stictiforme* bacterial communities. However, we also found inter- and intra-CCA morphotype differences in bacteria family composition, in line with results from other studies that observed dissimilarities in macroalgal bacteria communities at lower taxonomic levels (Hollants et al., 2013; Quinlan et al., 2019; Korlević et al., 2021). In our case, the differences were often due to the less abundant families *Thiohalorhabdaceae* and *Illumatobacteraceae*, and *Desulfobulbaceae* and NB1-j, uniquely associated with *L. stictiforme* and *Mesophyllum* sp., respectively, and unevenly

distributed among individuals of the same morphotype. However, we also found differences for two highly predominant bacteria families exclusively present in *L. stictiforme* individuals, namely *Spongiibacteriaceae* and *Stappiaceae*. Indeed, the first one was associated almost exclusively to CCAs of ST27, while the second presented high predominance only in clade C3. *Spongiibacteriaceae* are Gammaproteobacteria potentially able to use proteorhodopsin to exploit light as an additional energy source (Holert et al., 2018). This group was found in association to the CCA *Neogoniolithon trichotomum* in the Gulf of California at high temperature and silicate concentration (Valdespino-Castillo et al., 2021), and in Mediterranean sponges as steroid-degrading bacteria (Spring et al., 2015). Steroids may act as immune defense boosters under thermal stress and they may have anti-inflammatory, antioxidant and antifouling effects in corals (Kong et al., 2012; Dembitsky, 2023; Ochsenkühn et al., 2023). They can also be produced by the tropical CCA *Hydrolithon boergesenii* and act as potential inducers of coral larval settlement (Quinlan et al., 2023). *Stappiaceae* have been found associated with benthic organisms (e.g., sponges, corals, anemones), possessing genetic traits that hint to a possible role in sulfur cycling and dimethylsulfoniopropionate (DSMP) production, a scavenge ROS compound potential antioxidant, and in increased abundance in response to thermal stress (Couceiro et al., 2021; Heric et al., 2023). The reason why these two families were abundant in two of the three *L. stictiforme* sampling sites cannot be explained in our study. Based on earlier studies, we could hypothesize a relation between the CCA small-scale environmental conditions linked to light and nutrients availability, and the presence of localized stressors which led to the proliferation of these two taxa. Analyzing the bacterial community of individuals of *L. stictiforme* under different environmental conditions and conducting manipulative experiments may shed light on the possibility of using these bacteria taxa as indicators of the host health status.

At the ASV level, only 2.5% of the total ASVs were shared between CCA morphotypes. Noteworthy, no ASVs were shared between CCA-associated bacteria and bacteria present in the surrounding seawater, as reported in previous studies (Cavalcanti et al., 2014; Sneed et al., 2015; Gefen-Treves et al., 2021). The number of shared ASVs between individuals of the same CCA species was also low compared to previous studies (Miranda et al., 2013; Brodie et al., 2016; Valdespino-Castillo et al., 2021). In *L. stictiforme*, not only few ASVs were shared between taxonomic clades, but also between thalli of the same clade. The percentage of shared ASVs only increased (4.2-7.5%) when individuals collected from the same sampling sites were compared. These results suggest that the proximity between hosts could promote the development of more similar bacterial assemblages. We can hypothesize that this proximity effect could be due to micro-environmental conditions or to bacteria horizontal transfer events (Hester et al., 2016). These hypotheses need to be further investigated, for instance by specifically targeting these bacteria and analyzing the water close to the host surface.

Among the shared bacteria, we found some ASVs being uniquely associated to one CCA morphotype, but also some shared by individuals of the two morphotypes. These ASVs were similar to some earlier found in biofilms, but also in endolithic communities of marine outcrops or in sponges and seaweeds (see Table 2). ASVs of *Blastopirellula* and *Pir4_lineage* fell within the list of top five abundant ASVs of both CCA morphotypes. Planctomycetes are commonly associated with red algae being able to resist the action of several algal antimicrobial compounds and to live in biofilms taking advantage of the polysaccharides commonly produced by the algae, especially sulphated heteropolysaccharides (agars and carrageenans) (Lage & Bondoso, 2014; Wegner et al. 2013; Bergstrom et al., 2023). In particular, *Blastopirellula* and the *Pir4_lineage* can exploit such compounds thanks to sulfatase enzymes (Bondoso et al., 2017). Interestingly, sulfated

glucosaminoglycan, together with other glucosamine and galactose residues, can be produced by certain CCAs and act as potential triggers for coral larvae settlement and metamorphosis (Morse & Morse, 1991). Although these ASVs were not shared between the two CCA morphotypes, they were predominantly shared among individuals either of *L. stictiforme* and *Mesophyllum* sp. These findings provide a basis for future research on the role of CCA holobionts in settlement mechanisms of Mediterranean coral larvae.

5. Conclusions

Our results showed that both *Litophyllum stictiforme* and *Mesophyllum* sp. CCAs are bacterial diversity reservoirs, hosting not only highly diverse, but also holobiont-specific bacterial communities. Microbial community composition differed between CCA taxa, but also among thalli of the same CCA, probably due to exogenous factors acting at the scale of the single thallum. Nonetheless, we observed that, for a given morphotype, bacterial communities are more similar between neighboring thalli. This suggests an influence of environmental conditions at microscale and a potential host-to-host bacteria transfer among holobionts that are close to each other. All these hypotheses should be tested by studying the seasonal and spatial variability of bacterial communities and their variations under stress conditions both in the field and by manipulative experiments. Predominant bacteria genera affiliated to bacteria taxa described in tropical studies as potential positive players in coral larvae settlement mechanisms were found in both CCAs. These results rise the hypothesis of a possible positive interaction between CCAs and coral larvae mediated by bacteria also in the Mediterranean Sea.

Declaration of interests

The authors declare no competing interests.

Acknowledgments

EM was supported by the support of the European Union programme Marie Curie Actions through the project RESTORE [grant number 101062275] and the European Union's Horizon 2020 research and innovation programme, ASSEMBLE Plus project [grant number 730984].

CRedit authorship contribution statement

Elisabetta Manea - Conceptualization, Formal analysis, Investigation, Methodology, Visualization, Writing – original draft; **Lorenzo Bramanti** - Conceptualization, Investigation, Methodology, Writing - review & editing; **Laura Pezzolesi** - Conceptualization, Formal analysis, Investigation, Methodology, Visualization, Writing - review & editing; **Annalisa Falace** - Investigation, Methodology, Writing - review & editing; **Sara Kaleb** - Investigation, Methodology, Visualization, Writing - review & editing; **Lucia Bongiorni** – Conceptualization, Writing - review & editing; **Pierre E. Galand** – Conceptualization, Methodology, Writing - review & editing.

References

- Asnaghi, V., Thrush, S. F., Hewitt, J. E., Mangialajo, L., Cattaneo-Vietti, R., Chiantore, M., 2015. Colonisation processes and the role of coralline algae in rocky shore community dynamics. *J. Sea Res.*, 95, 132-138. doi.org/10.1016/j.seares.2014.07.012
- Ballesteros, E., 2006. Mediterranean coralligenous assemblages: A synthesis of present knowledge. *Oceanogr. Mar. Biol.: An Annual Review*, 44, 123–195.

- Barott, K. L., Rodriguez-Brito, B., Janouškovec, J., Marhaver, K. L., Smith, J. E., Keeling, P., Rohwer, F. L., 2011. Microbial diversity associated with four functional groups of benthic reef algae and the reef-building coral *Montastraea annularis*. *Environ. Microbiol.*, 13(5), 1192-1204. doi.org/10.1111/j.1462-2920.2010.02419.x
- Bengtsson, M.M., Sjötn, K., Lanzen, A., Ovreas, L., 2012. Bacterial diversity in relation to secondary production and succession on surfaces of the kelp *Laminaria hyperborea*. *ISME J.*, 6: 2188–2198. doi.org/10.1038/ismej.2012.67
- Bergstrom, E., Lahnstein, J., Collins, H., Page, T. M., Bulone, V., Diaz-Pulido, G., 2023. Cell wall organic matrix composition and biomineralization across reef-building coralline algae under global change. *J. Phycol.*, 59(1), 111-125. DOI: 10.1111/jpy.13290
- Bittner, L., Halary, S., Payri, C., Cruaud, C., de Reviers, B., Lopez, P., Bapteste, E., 2010. Some considerations for analyzing biodiversity using integrative metagenomics and gene networks. *Biol. Direct*, 5(1), 1-17. doi.org/10.1186/1745-6150-5-47
- Bondoso, J., Godoy-Vitorino, F., Balague, V., Gasol, J. M., Harder, J., Lage, O. M., 2017. Epiphytic Planctomycetes communities associated with three main groups of macroalgae. *FEMS Microbiol. Ecol.*, 93(3), fiw255. doi.org/10.1093/femsec/fiw255
- Bracchi, V. A., Bazzicalupo, P., Fallati, L., Varzi, A. G., Savini, A., Negri, M. P., et al., 2022. The main builders of Mediterranean coralligenous: 2D and 3D quantitative approaches for its identification. *Front. Earth Sci.*, 10, 910522. doi.org/10.3389/feart.2022.910522
- Bramanti, L., Rossi, S., Tsounis, G., Gili, J. M., Santangelo, G., 2007. Settlement and early survival of red coral on artificial substrates in different geographic areas: some clues for demography and restoration. *Hydrobiologia*, 580, 219-224. doi.org/10.1007/s10750-006-0452-1

- Bramanti, L., Manea, E., Giordano, B., Estaque, T., Bianchimani, O., Richaume, J., et al., 2023. The deep vault: a temporary refuge for temperate gorgonian forests facing marine heat waves. *Mediterr. Mar. Sci.*, 24(3), 601-609. doi: 10.12681/mms.35564
- Brodie, J., Williamson, C., Barker, G. L., Walker, R. H., Briscoe, A., Yallop, M., 2016. Characterising the microbiome of *Corallina officinalis*, a dominant calcified intertidal red alga. *FEMS Microbiol. Ecol.*, 92(8), fiw110. doi.org/10.1093/femsec/fiw110
- Broom, J. E. S., Hart, D. R., Farr, T. J., Nelson, W. A., Neill, K. F., Harvey, A. S., Woelkerling, W. J., 2008. Utility of *psbA* and nSSU for phylogenetic reconstruction in the Corallinales based on New Zealand taxa. *Mol. Phylogen. Evol.* 46, 958– 73. doi.org/10.1016/j.ympev.2007.12.016
- Burke, C., Steinberg, P., Rusch, D., Kjelleberg, S., Thomas, T., 2011. Bacterial community assembly based on functional genes rather than species. *Proc. Natl. Acad. Sci. U.S.A.*, 108(34), 14288-14293. doi.org/10.1073/pnas.110159110
- Callahan, B. J., McMurdie, P. J., Rosen, M. J., Han, A. W., Johnson, A. J. A., Holmes, S. P., 2016. DADA2: high-resolution sample inference from Illumina amplicon data. *Nat. Methods*, 13, 581–583. doi: 10.1038/nmeth.3869
- Casoli, E., Ventura, D., Mancini, G., Cardone, S., Farina, F., Donnini, L., et al., 2022. Rehabilitation of Mediterranean animal forests using gorgonians from fisheries by-catch. *Restor. Ecol.*, 30(1), e13465. doi.org/10.1111/rec.13465
- Castellan, G., Angeletti, L., Montagna, P., Taviani, M., 2022. Drawing the borders of the mesophotic zone of the Mediterranean Sea using satellite data. *Sci. Rep.*, 12, 5585. doi.org/10.1038/s41598-022-09413-4

- Cavalcanti, G. S., Gregoracci, G. B., Dos Santos, E. O., Silveira, C. B., Meirelles, P. M., Longo, L., et al., 2014. Physiologic and metagenomic attributes of the rhodoliths forming the largest CaCO₃ bed in the South Atlantic Ocean. *ISME J.*, 8(1), 52-62. doi.org/10.1038/ismej.2013.133
- Chatzimentor, A., Doxa, A., Katsanevakis, S., Mazaris, A. D., 2023. Are Mediterranean marine threatened species at high risk by climate change?. *Glob. Change Biol.*, 29(7), 1809-1821. doi.org/10.1111/gcb.16577
- Cornwall, C. E., Harvey, B. P., Comeau, S., Cornwall, D. L., Hall-Spencer, J. M., Peña, V., et al., 2022. Understanding coralline algal responses to ocean acidification: Meta-analysis and synthesis. *Glob. Change Biol.*, 28(2), 362-374. doi.org/10.1111/gcb.15899
- Couceiro, J. F., Keller-Costa, T., Marques, M., Kyrpides, N. C., Woyke, T., Whitman, W. B., Costa, R., 2021. The *Roseibium album* (*Labrenzia alba*) genome possesses multiple symbiosis factors possibly underpinning host-microbe relationships in the marine benthos. *Microbiol. Resour. Announc.*, 10(34), 10-1128. doi.org/10.1128/mra.00320-21
- Dembitsky, V. M., 2023. Biological Activity and Structural Diversity of Steroids Containing Aromatic Rings, Phosphate Groups, or Halogen Atoms. *Molecules*, 28(14), 5549. doi.org/10.3390/molecules28145549
- De Jode, A., David, R., Haguenaer, A., Cahill, A. E., Erga, Z., Guillemain, D., et al., 2019. From seascape ecology to population genomics and back. Spatial and ecological differentiation among cryptic species of the red algae *Lithophyllum stictiforme*/*L. cabiochia*, main bioconstructors of coralligenous habitats. *Mol. Phylogenetics Evol.*, 137, 104-113. doi.org/10.1016/j.ympev.2019.04.005

- Garrabou, J., Gómez-Gras, D., Medrano, A., Cerrano, C., Ponti, M., Schlegel, R., et al., 2022. Marine heatwaves drive recurrent mass mortalities in the Mediterranean Sea. *Glob. Change Biol.*, 28(19), 5708-5725. doi.org/10.1111/gcb.16301
- Gefen-Treves, S., Bartholomäus, A., Horn, F., Zaborowski, A. B., Tchernov, D., Wagner, D., et al., 2021. The microbiome associated with the reef builder *Neogoniolithon* sp. in the eastern Mediterranean. *Microorganisms*, 9(7), 1374. doi.org/10.3390/microorganisms9071374
- Glasl, B., Webster, N. S., Bourne, D. G., 2017. Microbial indicators as a diagnostic tool for assessing water quality and climate stress in coral reef ecosystems. *Mar. Biol.*, 164, 1-18. doi.org/10.1007/s00227-017-3097-x
- Gómez-Lemos, L.A., Diaz-Pulido, G., 2017. Crustose coralline algae and associated microbial biofilms deter seaweed settlement on coral reefs. *Coral Reefs*, 36, 453–462. <https://doi.org/10.1007/s00338-017-1549-x>
- Gómez-Lemos, L. A., Doropoulos, C., Bayraktarov, E., Diaz-Pulido, G., 2018. Coralline algal metabolites induce settlement and mediate the inductive effect of epiphytic microbes on coral larvae. *Sci. Rep.*, 8(1), 17557. doi.org/10.1038/s41598-018-35206-9
- Guiry, M. D., Guiry, G. M., 2023. AlgaeBase. World-wide electronic publication, National University of Ireland, Galway. Available at <http://www.algaebase.org> (accessed 22 November 2023).
- Heric, K., Maire, J., Deore, P., Perez-Gonzalez, A., van Oppen, M. J., 2023. Inoculation with *Roseovarius* increases thermal tolerance of the coral photosymbiont, *Breviolum minutum*. *Front. Ecol. Evol.*, 11. doi.org/10.3389/fevo.2023.1079271

- Hereu, B., Kersting, D. K., 2016. Diseases of coralline algae in the Mediterranean Sea. *Coral reefs*, 35(2), 713-713. DOI 10.1007/s00338-016-1428-x
- Hester, E. R., Barott, K. L., Nulton, J., Vermeij, M. J., Rohwer, F. L., 2016. Stable and sporadic symbiotic communities of coral and algal holobionts. *ISME J.*, 10(5), 1157-1169. doi.org/10.1038/ismej.2015.190
- Holert, J., Cardenas, E., Bergstrand, L. H., Zaikova, E., Hahn, A. S., Hallam, S. J., Mohn, W. W., 2018. Metagenomes reveal global distribution of bacterial steroid catabolism in natural, engineered, and host environments. *MBio*, 9(1), 10-1128. doi.org/10.1128/mbio.02345-17
- Hollants, J., Leliaert, F., De Clerck, O., Willems, A., 2013. What we can learn from sushi: a review on seaweed–bacterial associations. *FEMS Microbiol. Ecol.*, 83(1), 1-16. doi.org/10.1111/j.1574-6941.2012.01446.x
- Iborra, L., Leduc, M., Fullgrabe, L., Cuny, P., Gobert, S., 2022. Temporal trends of two iconic Mediterranean gorgonians (*Paramuricea clavata* and *Eunicella cavolini*) in the climate change context. *J. Sea Res.*, 186, 102241. doi.org/10.1016/j.seares.2022.102241
- Jorissen, H., Galand, P. E., Bonnard, I., Meiling, S., Raviglione, D., Meistertzheim, A. L., et al., 2021. Coral larval settlement preferences linked to crustose coralline algae with distinct chemical and microbial signatures. *Sci. Rep.*, 11(1), 14610. doi.org/10.1038/s41598-021-94096-6
- Kaleb, S., Falace, A., Sartoni, G., Woelkelring, W.J., 2011. Morphology-anatomy of *Mesophyllum macroblastum* (Hapalidiaceae, Corallinales, Rhodophyta) in the Northern Adriatic Sea and a key to Mediterranean species of the genus. *Cryptogam., Algol.*, 32, 223–242. doi.org/10.7872/crya.v32.iss3.2011.223

- Kaleb, S., Alongi, G., Falace, A., 2018. Coralline algae preparation for scanning electron microscopy and optical microscopy. in: Charrier, B., Wichard, T. & Reddy, C. R. K. (Eds.) *Protocols for Macroalgae Research*. CRC Press, Taylor & Francis, Boca Raton, Florida, pp. 413–29.
- Klindworth, A., Pruesse, E., Schweer, T., Peplies, J., Quast, C., Horn, M., Glöckner, F. O., 2013. Evaluation of general 16S ribosomal RNA gene PCR primers for classical and next-generation sequencing-based diversity studies. *Nucleic Acids Res.*, *41*(1), e1-e1. doi.org/10.1093/nar/gks808
- Kong, W.W., Shao, C.L., Wang, C.Y., Xu, Y., Qian, P.Y., Chen, A.N., Huang, H., 2012. Diterpenoids and steroids from Gorgonian *Subergorgia mollis*. *Chem. Nat. Compd.*, *48*, 512–515. doi:10.1007/s10600-012-0294-1
- Korlević, M., Markovski, M., Zhao, Z., Herndl, G. J., Najdek, M., 2021. Seasonal dynamics of epiphytic microbial communities on marine macrophyte surfaces. *Front. microbiol.*, *12*, 671342. doi.org/10.3389/fmicb.2021.671342
- Lage, O. M., Bondoso, J., 2014. Planctomycetes and macroalgae, a striking association. *Front. Microbiol.*, *5*, 267. doi.org/10.3389/fmicb.2014.00267
- Lahti, L., Shetty, S. et al., 2017. Tools for microbiome analysis in R. Version . URL: <http://microbiome.github.com/microbiome>.
- Larsson, A., 2014. AliView: a fast and lightweight alignment viewer and editor for large datasets. *Bioinformatics*, *30*(22), 3276-3278. doi.org/10.1093/bioinformatics/btu531

- Lau, S. C., Thiyagarajan, V., Cheung, S. C., Qian, P. Y., 2005. Roles of bacterial community composition in biofilms as a mediator for larval settlement of three marine invertebrates. *Aquat. Microb. Ecol.*, 38(1), 41-51. doi:10.3354/ame038041
- Linares, C., Coma, R., Zabala, M., 2008. Restoration of threatened red gorgonian populations: an experimental and modelling approach. *Biol. Conserv.*, 141(2), 427-437. doi.org/10.1016/j.biocon.2007.10.012
- Martin, S., Gattuso, J. P., 2009. Response of Mediterranean coralline algae to ocean acidification and elevated temperature. *Glob. Change Biol.*, 15(8), 2089-2100. doi.org/10.1111/j.1365-2486.2009.01874.x
- Martin, C. S., Giannoulaki, M., De Leo, F., Scardi, M., Salomidi, M., Knittweis, L., et al., 2014. Coralligenous and maërl habitats: predictive modelling to identify their spatial distributions across the Mediterranean Sea. *Sci. Rep.*, 4(1), 5073. doi.org/10.1038/srep05073
- McLaren, M. R., Callahan, B. J., 2021. Silva 138.1 prokaryotic SSU taxonomic training data formatted for DADA2 [Data set]. Zenodo. doi.org/10.5281/zenodo.4587955
- McMurdie, P. J., Holmes, S., 2013. phyloseq: an r package for reproducible interactive analysis and graphics of microbiome census data. *PLoS One*, 8:e61217. doi: 10.1371/journal.pone.0061217
- Miranda, L. N., Hutchison, K., Grossman, A. R., Brawley, S. H., 2013. Diversity and abundance of the bacterial community of the red macroalga *Porphyra umbilicalis*: did bacterial farmers produce macroalgae?. *PLoS One*, 8(3), e58269. doi.org/10.1371/journal.pone.0058269

- Montseny, M., Linares, C., Viladrich, N., Olariaga, A., Carreras, M., Palomeras, N., et al., 2019. First attempts towards the restoration of gorgonian populations on the Mediterranean continental shelf. *Aquat. Conserv.: Mar. Freshw. Ecosyst.*, 29(8), 1278-1284. doi.org/10.1002/aqc.3118
- Morse, D. E., Morse, A. N., 1991. Enzymatic characterization of the morphogen recognized by *Agaricia humilis* (scleractinian coral) larvae. *Biol. Bull.*, 181(1), 104-122. doi.org/10.2307/1542493
- Nei M., Kumar S., 2000. *Molecular Evolution and Phylogenetics*. Oxford University Press, New York.
- Ochsenkühn, M., Mohamed, A. R., Haydon, T. D., Coe, L. S., Abrego, D., Amin, S. A., 2023. Endozoicomonas provides corals with steroid hormones during thermal stress. *bioRxiv*, 2023-09.
- Oksanen, J., Blanchet, F. G., Friendly, M., Kindt, R., Legendre, P., McGlinn, D., et al., 2013. Vegan: Community Ecology Package. R Package Version. 2.5–2.
- O’Leary, J. K., Barry, J. P., Gabrielson, P. W., Rogers-Bennett, L., Potts, D. C., Palumbi, S. R., Micheli, F., 2017. Calcifying algae maintain settlement cues to larval abalone following algal exposure to extreme ocean acidification. *Sci. Rep.*, 7(1), 1-10. DOI:10.1038/s41598-017-05502-x
- Peña, V., De Clerck, O., Afonso-Carrillo, J., Ballesteros, E., Bárbara, I., Barreiro R., Le Gall L., 2015. An integrative systematic approach to species diversity and distribution in the genus *Mesophyllum* (Corallinales, Rhodophyta) in Atlantic and Mediterranean Europe. *Eur. J. Phycol.*, 50(1), 20-36, DOI: 10.1080/09670262.2014.981294

- Pezzolesi, L., Falace, A., Kaleb, S., Hernandez-Kantun, J. J., Cerrano, C., Rindi, F., 2017. Genetic and morphological variation in an ecosystem engineer, *Lithophyllum byssoides* (Corallinales, Rhodophyta). *J. Phycol.*, 53(1), 146-160. doi.org/10.1111/jpy.12837
- Pezzolesi, L., Peña, V., Le Gall, L., Gabrielson, P. W., Kaleb, S., Hughey, J. R., et al., 2019. Mediterranean *Lithophyllum stictiforme* (Corallinales, Rhodophyta) is a genetically diverse species complex: implications for species circumscription, biogeography and conservation of coralligenous habitats. *J. Phycol.*, 55(2), 473-492. doi.org/10.1111/jpy.12837
- Piazzzi, L., Pinna, F., Ceccherelli, G., 2022. Crustose coralline algae and biodiversity enhancement: The role of *Lithophyllum stictiforme* in structuring Mediterranean coralligenous reefs. *Estuar. Coast. Shelf Sci.*, 278, 108121. doi.org/10.1016/j.ecss.2022.108121
- Quéré, G., Intertaglia, L., Payri, C., Galand, P. E., 2019. Disease specific bacterial communities in a Coralline Algae of the Northwestern Mediterranean Sea: A combined culture dependent and-independent approach. *Front. Microbiol.*, 10, 1850. doi.org/10.3389/fmicb.2019.01850
- Quinlan, Z. A., Ritson-Williams, R., Carroll, B. J., Carlson, C. A., Nelson, C. E., 2019. Species-specific differences in the microbiomes and organic exudates of crustose coralline algae influence bacterioplankton communities. *Front. Microbiol.*, 10, 2397. doi.org/10.3389/fmicb.2019.02397
- Quinlan, Z. A., Bennett, M. J., Arts, M. G., Levenstein, M., Flores, D., Tholen, H. M., et al., 2023. Coral larval settlement induction using tissue-associated and exuded coralline algae metabolites and the identification of putative chemical cues. *Proc. R. Soc. B*, 290(2009), 20231476. doi.org/10.1098/rspb.2023.1476

- Rindi, F., Braga, J. C., Martin, S., Peña, V., Le Gall, L., Caragnano, A., Aguirre, J., 2019. Coralline algae in a changing Mediterranean Sea: how can we predict their future, if we do not know their present?. *Front. Mar. Sci.*, 6, 723. doi.org/10.3389/fmars.2019.00723
- Saitou N., Nei M., 1987. The neighbor-joining method: A new method for reconstructing phylogenetic trees. *Mol. Biol. Evol.*, 4, 406-425.
- Salonen, A., Salojärvi, J., Lahti, L., de Vos, W. M., 2012. The adult intestinal core microbiota is determined by analysis depth and health status. *Clin. Microbiol. Infect.*, 18, 16-20. doi.org/10.1111/j.1469-0691.2012.03855.x
- Seabra, M., Cruz, T., Fernandes, J., Silva, T., Hawkins, S., 2019. Recruitment of the limpet *Patella ulyssiponensis* and its relationship with crustose coralline algae: Patterns of juvenile distribution and larval settlement. *J. Mar. Biolog. Assoc. U.K.*, 99(8), 1787-1796. doi:10.1017/S0025315419000869
- Short, J., Foster, T., Falter, J., Kendrick, G. A., McCulloch, M. T., 2015. Crustose coralline algal growth, calcification and mortality following a marine heatwave in Western Australia. *Cont. Shelf Res.* 106, 38-44. doi.org/10.1016/j.csr.2015.07.003
- Siboni, N., Abrego, D., Puill-Stephan, E., King, W. L., Bourne, D. G., Raina, J. B., et al., 2020. Crustose coralline algae that promote coral larval settlement harbor distinct surface bacterial communities. *Coral Reefs*, 39, 1703-1713. doi.org/10.1007/s00338-020-01997-5
- Singh, R. P., Reddy, C. R. K., 2016. Unraveling the functions of the macroalgal microbiome. *Front. Microbiol.*, 6, 1488. doi.org/10.3389/fmicb.2015.01488

- Singh, R.P., Kothari, R., Egan, S., 2017. Exploring the Complexity of Macroalgal-Bacterial Interactions Through Interkingdom Signalling System. in: Kumar, M., Ralph, P. (Eds) Systems Biology of Marine Ecosystems. Springer, Cham. doi.org/10.1007/978-3-319-62094-7_15
- Sneed, J. M., Ritson-Williams, R., Paul, V. J., 2015. Crustose coralline algal species host distinct bacterial assemblages on their surfaces. *ISME J.*, 9(11), 2527-2536. doi.org/10.1038/ismej.2015.67
- Spring, S., Scheuner, C., Göker, M., Klenk, H. P., 2015. A taxonomic framework for emerging groups of ecologically important marine gammaproteobacteria based on the reconstruction of evolutionary relationships using genome-scale data. *Front. Microbiol.*, 6, 281. doi.org/10.3389/fmicb.2015.00281
- Staufenberger, T., Thiel, V., Wiese, J., Imhoff, J. F., 2008. Phylogenetic analysis of bacteria associated with *Laminaria saccharina*. *FEMS Microbiol. Ecol.*, 64(1), 65-77. doi.org/10.1111/j.1574-6941.2008.00445.x
- Tamura K., Stecher G., Kumar S., 2021. MEGA 11: Molecular Evolutionary Genetics Analysis Version 11. *Mol. Biol. Evol.*. doi.org/10.1093/molbev/msab120.
- Tignat-Perrier, R., van de Water, J. A., Guillemain, D., Aurelle, D., Allemand, D., Ferrier-Pagès, C., 2022. The effect of thermal stress on the physiology and bacterial communities of two key Mediterranean gorgonians. *Appl. Environ. Microbiol.*, 88(6), e02340-21. doi.org/10.1128/aem.02340-21
- Toma, M., Bo, M., Cattaneo-Vietti, R., Canese, S., Canessa, M., Cannas, R., et al., 2022. Basin-scale occurrence and distribution of mesophotic and upper bathyal red coral forests along the Italian coasts. *Mediterr. Mar. Sci.*, 23(3), 484-498. doi: 10.12681/mms.28052

- Valdespino-Castillo, P. M., Bautista-García, A., Favoretto, F., Merino-Ibarra, M., Alcántara-Hernández, R. J., Pi-Puig, T., et al., 2021. Interplay of microbial communities with mineral environments in coralline algae. *Sci. Total Environ.*, 757, 143877. doi.org/10.1016/j.scitotenv.2020.143877

- Vitelletti, M. L., Manea, E., Bongiorni, L., Ricchi, A., Sangelantoni, L., Bonaldo, D., 2023. Modelling distribution and fate of coralligenous habitat in the Northern Adriatic Sea under a severe climate change scenario. *Front. Mar. Sci.*, 10, 88. doi.org/10.3389/fmars.2023.1050293

- Wegner, C. E., Richter-Heitmann, T., Klindworth, A., Klockow, C., Richter, M., Achstetter, T., et al., 2013. Expression of sulfatases in *Rhodopirellula baltica* and the diversity of sulfatases in the genus *Rhodopirellula*. *Mar. Genomics*, 9, 51-61. doi.org/10.1016/j.margen.2012.12.001

- Yang, F., Mo, J., Wei, Z., Long, L., 2021. Calcified macroalgae and their bacterial community in relation to larval settlement and metamorphosis of reef-building coral *Pocillopora damicornis*. *FEMS Microbiol. Ecol.*, 97(1), fiae215. doi.org/10.1093/femsec/fiae215

- Zelli, E., Quéré, G., Lago, N., Di Franco, G., Costantini, F., Rossi, S., Bramanti, L., 2020. Settlement dynamics and recruitment responses of Mediterranean gorgonians larvae to different crustose coralline algae species. *J. Exp. Mar. Bio. Ecol.*, 530, 151427. doi.org/10.1016/j.jembe.2020.151427

Figures and Table

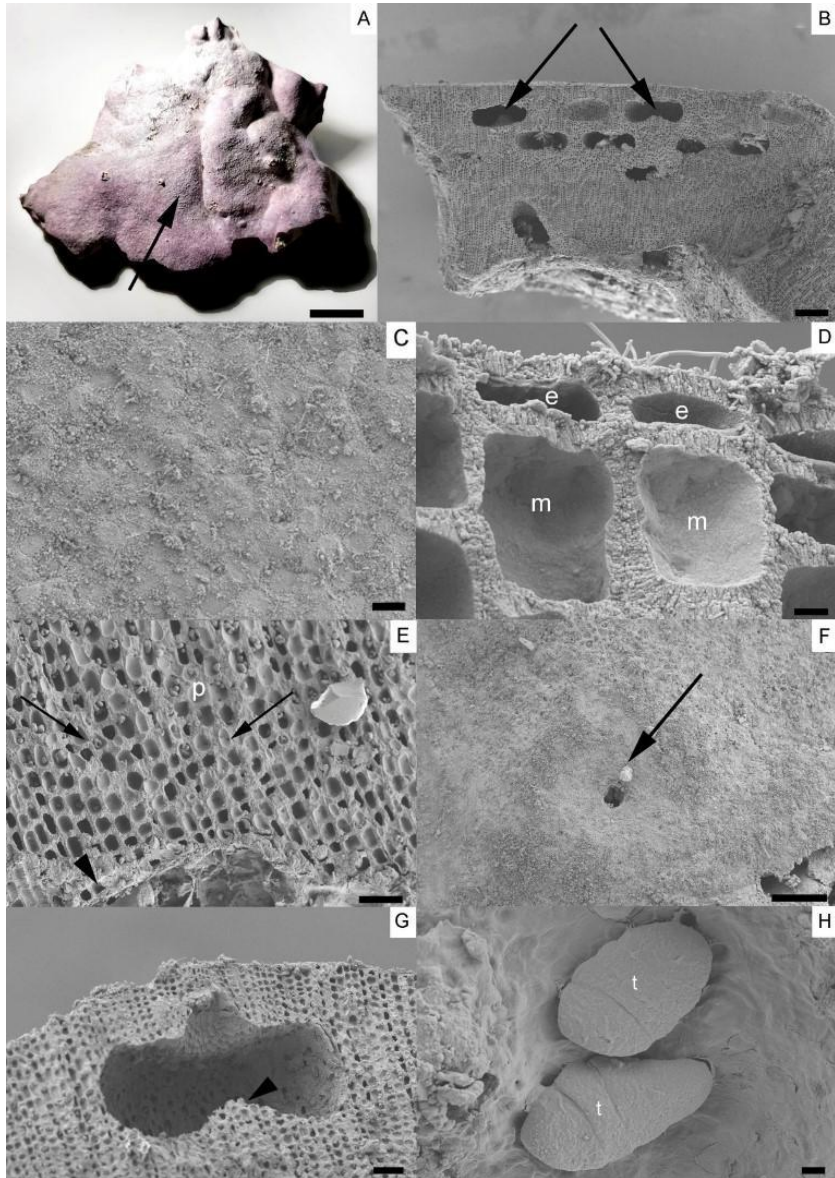


Figure 1. Morphotype 1 - *Lithophyllum stictiforme* samples from stations ST7 and ST27. **A.** Specimen with flat surface and uniporate conceptacles (arrow). Scale bar = 1 cm. **B.** Longitudinal section of a thallus with old buried dumbbell-shaped conceptacles (arrows). Scale bar = 200 μm . **C.** Abraded epithallus in surface view. The cells are not easily distinguishable. Scale bar = 5 μm . **D.** Epithallial cells (e) with slightly convex distal cell wall and rectangular meristematic cells (m). Scale bar = 2 μm . **E.** Peripheral filaments with cells joined laterally by secondary pit connections (arrows) and monostromatic ventral region (arrowhead). Scale bar = 30 μm . **F.** Slightly protruding uniporate conceptacle in surface (arrow). Scale bar = 100 μm . **G.** Section through a tetrasporangial conceptacle with a prominent central columella (arrowhead). Scale bar = 40 μm . **H.** Detail of tetrasporangia (t) lying on the wall of a conceptacle. Scale bar = 10 μm .

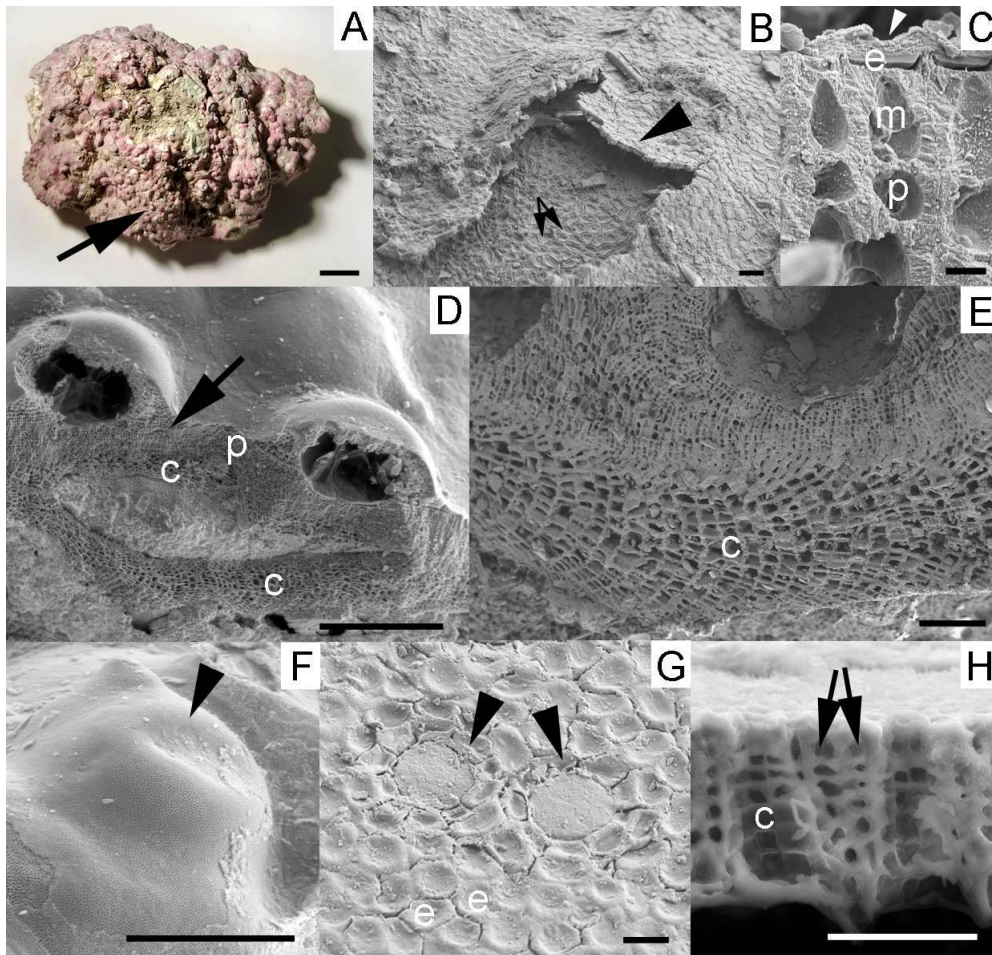


Figure 2. Morphotype 2 – *Mesophyllum* sp. **A.** Specimen with encrusting to warty growth form and grouped multiporate conceptacles. Scale bar = 5 mm. **B.** Epitallus in surface view. Note flared epithallial cells (arrows) and a large area with shedding epithallial cells (arrowhead). Scale bar = 20 μ m. **C.** Section with a flared epithallial cell (e) subtended by a meristematic cell (m) longer than the subtending peripheral cell (p). Scale bar = 4 μ m. **D.** Section of a thallus with multiporate conceptacles protruding above the thallus surface, with the chamber floor 10-12 cells deep into the peripheral region (p), and not in contact with the core (c). Scale bar = 500 μ m. **E.** Detail of the coaxial core (c) with cells of adjacent filaments aligned in arching tiers. Scale bar = 100 μ m. **F.** A multiporate conceptacle with a rim (arrowhead) and a slightly sunken pore plate. Scale bar = 500 μ m. **G.** Surface view of a conceptacle showing pores bordered by cells (arrowheads) smaller than the other epithallial roof cells (e). Scale bar = 300 μ m. **H.** Section of a conceptacle roof plate showing the cells (c) lining the pore canals. In the central and basal part of the pore canal the lining cells are square and larger than the other plate cells.

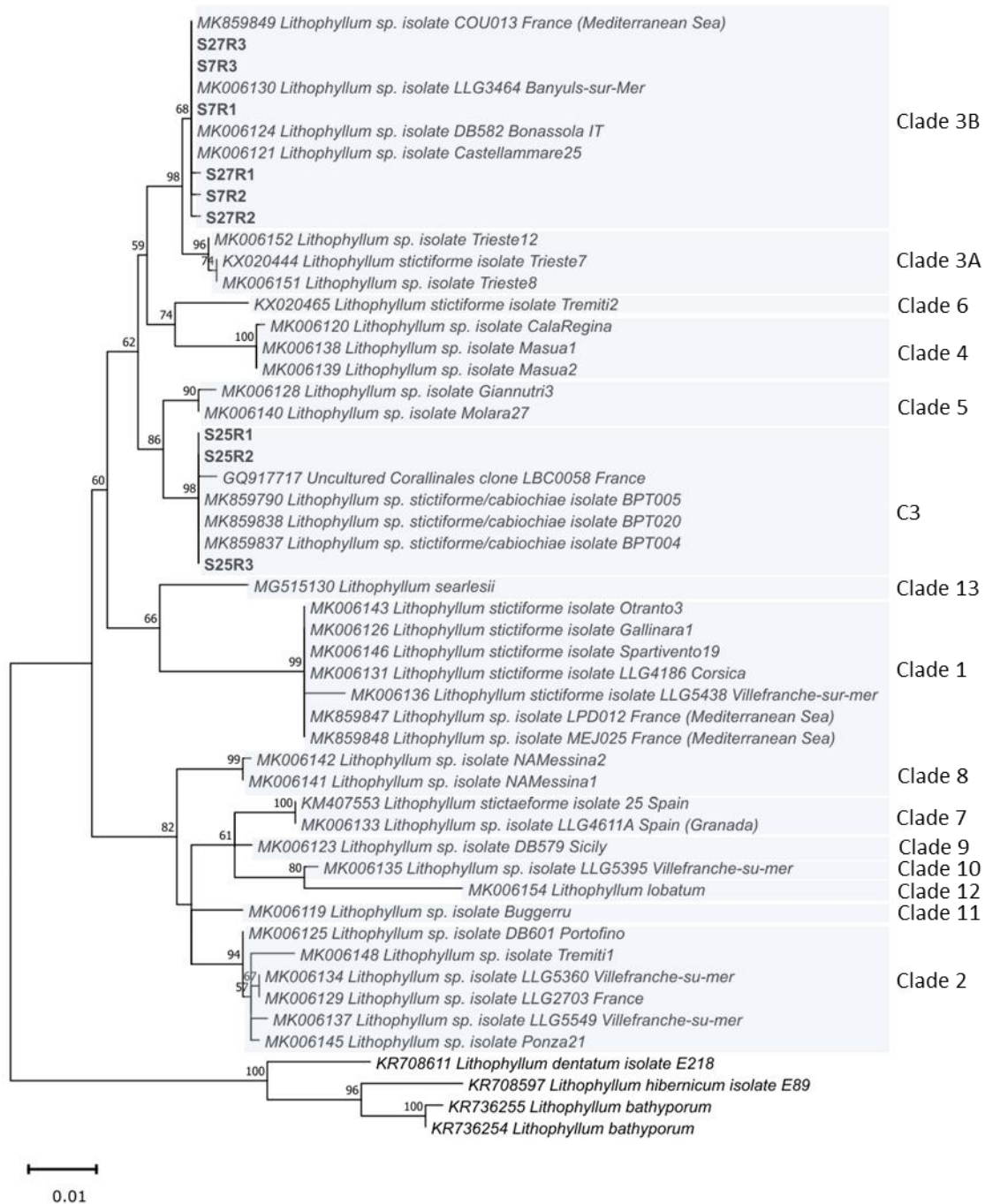


Figure 3. *Lithophyllum stictiforme* phylogenetic tree. Phylogenetic tree inferred from ML analysis of the psbA sequences of Mediterranean *Lithophyllum stictiforme* and other publicly available sequences for this complex. Bootstrap ML values > 60% are shown for each node. *L. dentatum*, *L. hibernicum* and *L. bathyporum* were used as outgroup. Clades 1 to 13 refer to the classification provided by Pezzolesi et al. (2019), while C3 corresponds to the haplotype identified by de Jode et al. (2019). Scale bar: 0.01 substitutions per site. Sequences generated in the present work are marked in bold.

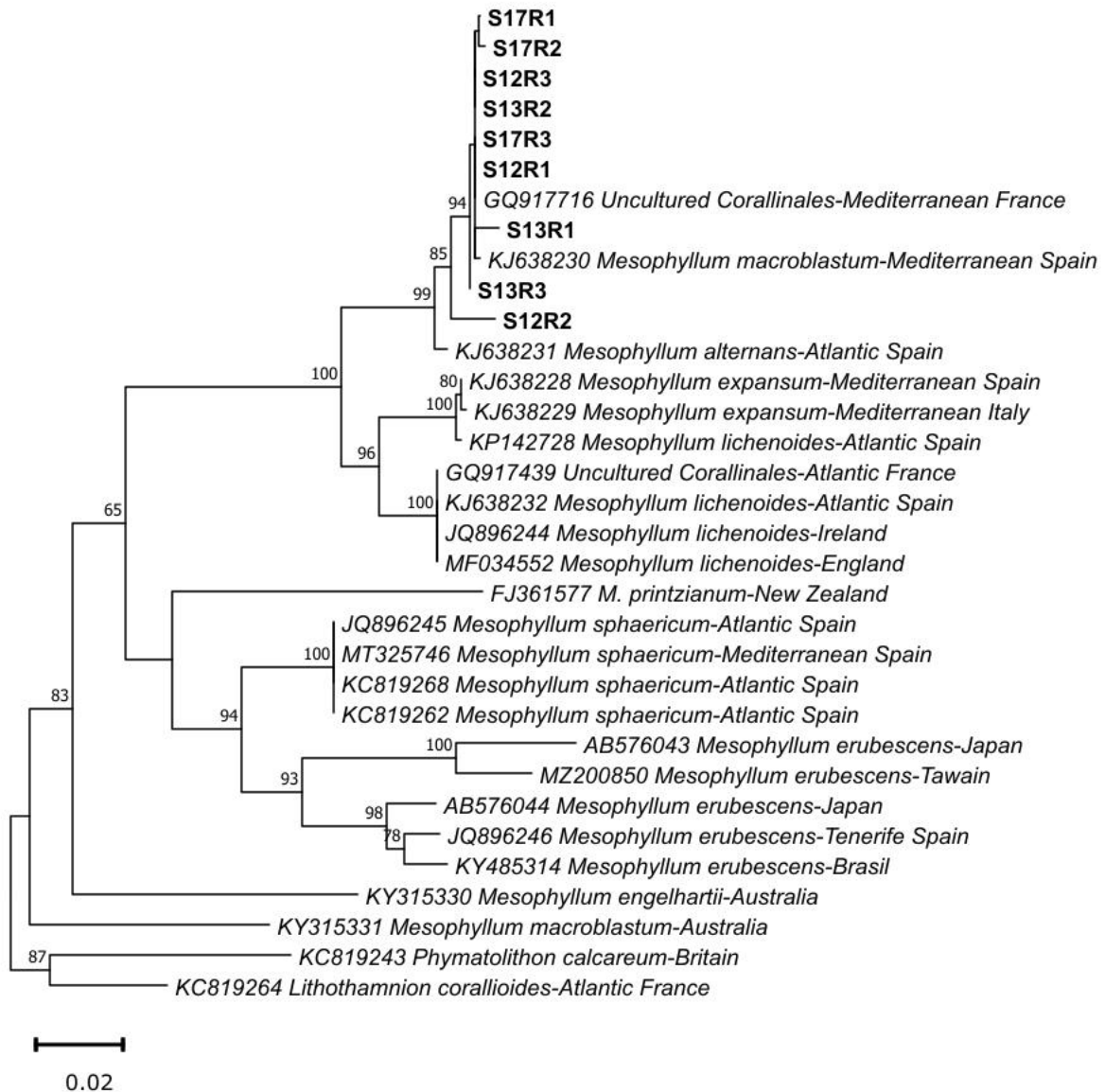


Figure 4. *Mesophyllum* sp. phylogenetic tree of the psbA sequences. Phylogenetic tree inferred from ML analysis of the psbA sequences of Mediterranean *Mesophyllum* and other publicly available sequences for this genus. Bootstrap ML values > 60% are shown for each node. Members of the subfamily Melobesioideae were used as outgroup. Scale bar: 0.02 substitutions per site. Sequences generated in the present work are marked in bold.

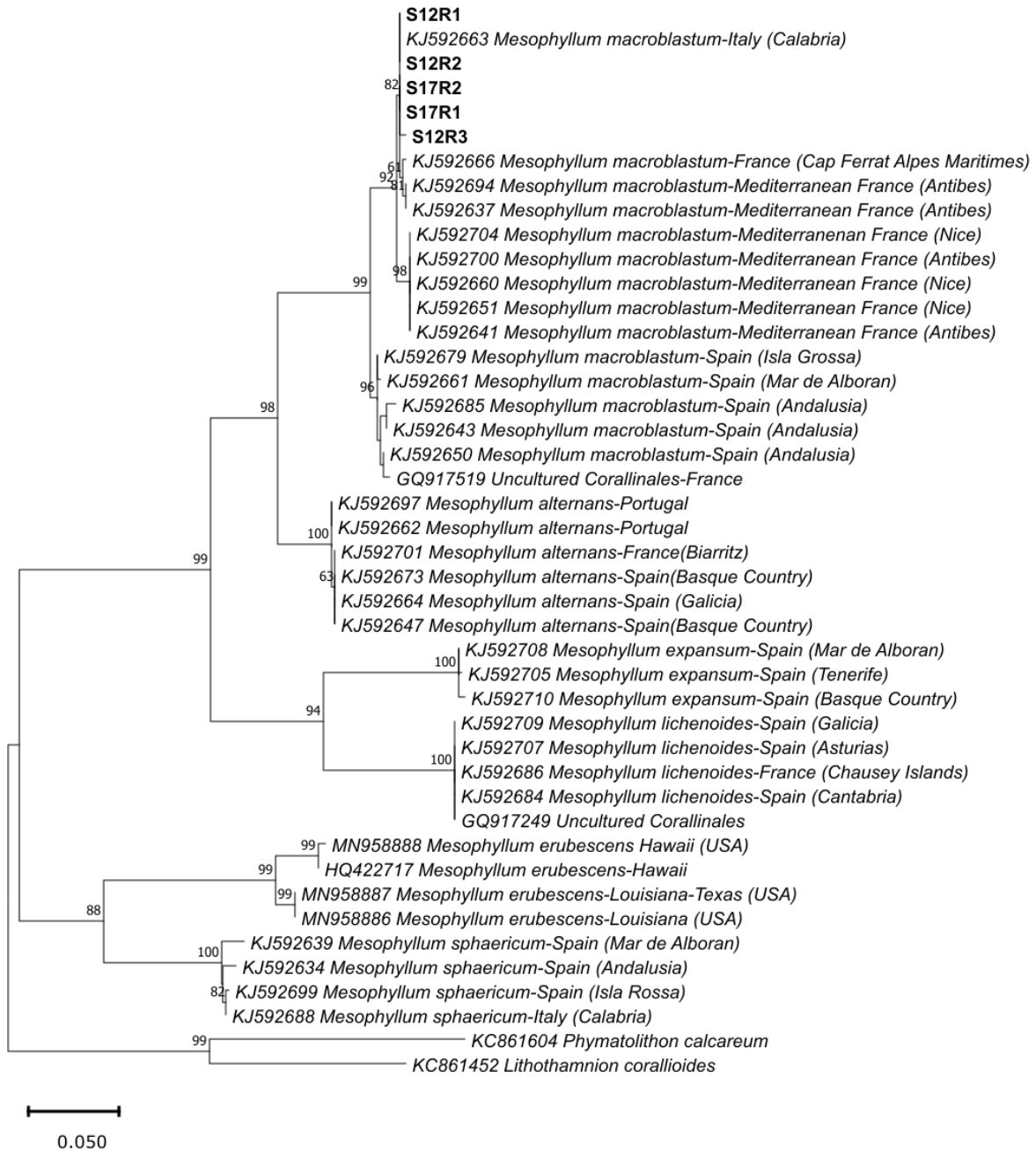


Figure 5. *Mesophyllum* sp. phylogenetic tree of the COI-5P sequences. Maximum likelihood tree inferred from the DNA barcode sequences (COI-5P) of morphotype 2 samples from stations S12 (R1-R3) and S17 (R1-R2), and other publicly available sequences for this genus. Bootstrap values > 60% between the species of *Mesophyllum* are shown for each node. Members of the subfamily Melobesioideae were used as outgroup. Scale bar: 0.05 substitutions per site. Sequences generated in the present work are marked in bold.

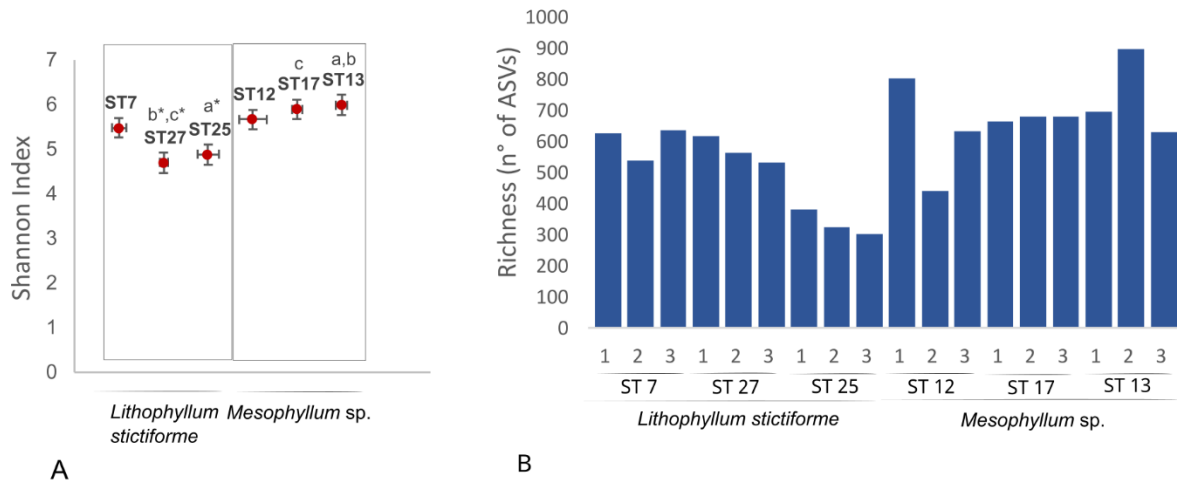


Figure 6. Diversity bacterial communities associated with the CCA *Lithophyllum stictiforme* and *Mesophyllum sp.* **A.** Mean value of the Shannon index for each sampling site. Significant differences are reported (p -value $< 0.05^*$). **B.** Richness (observed number of ASVs) of each individual CCA bacterial community.

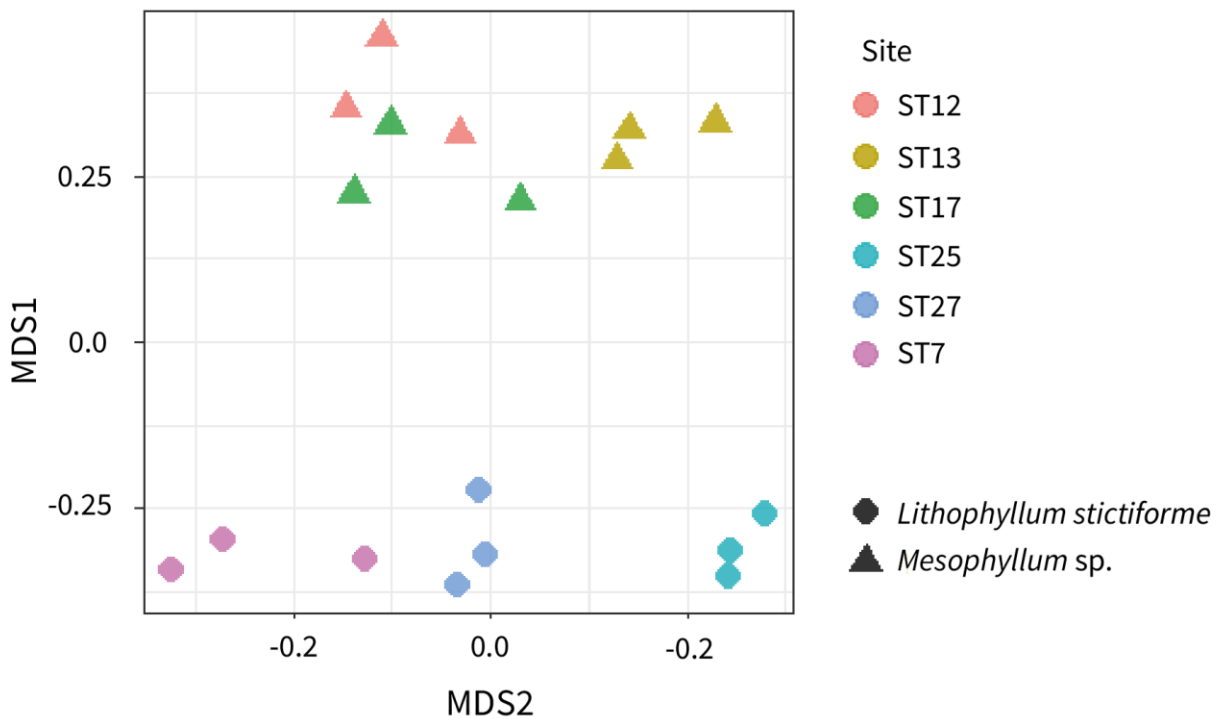
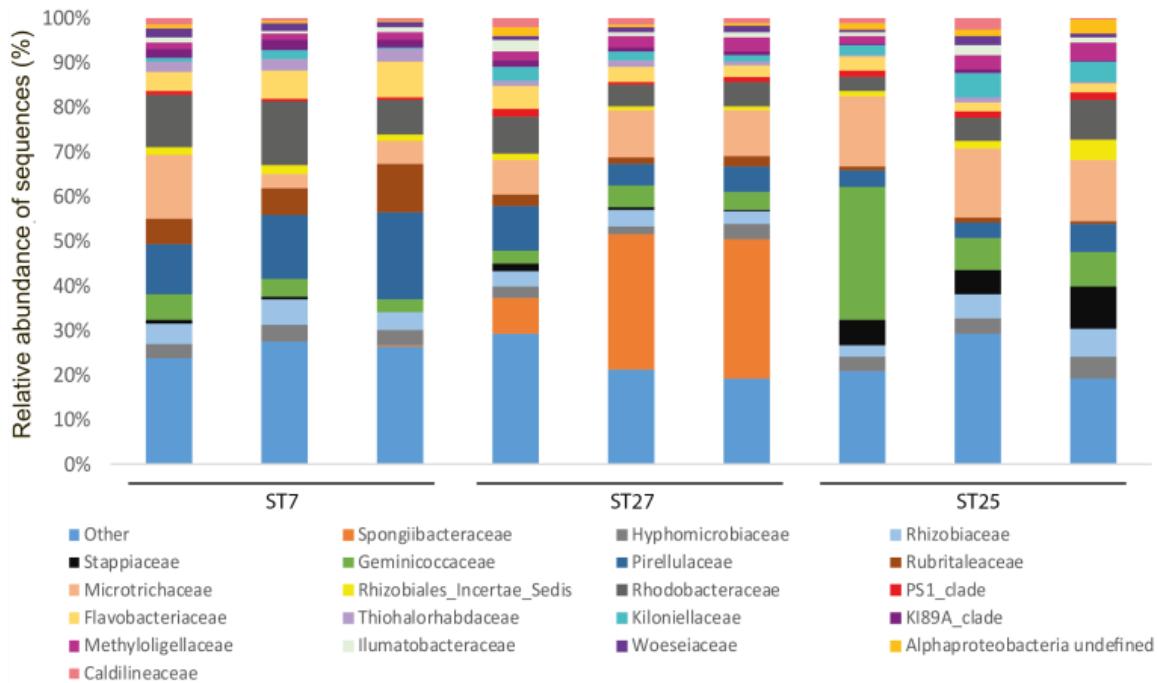
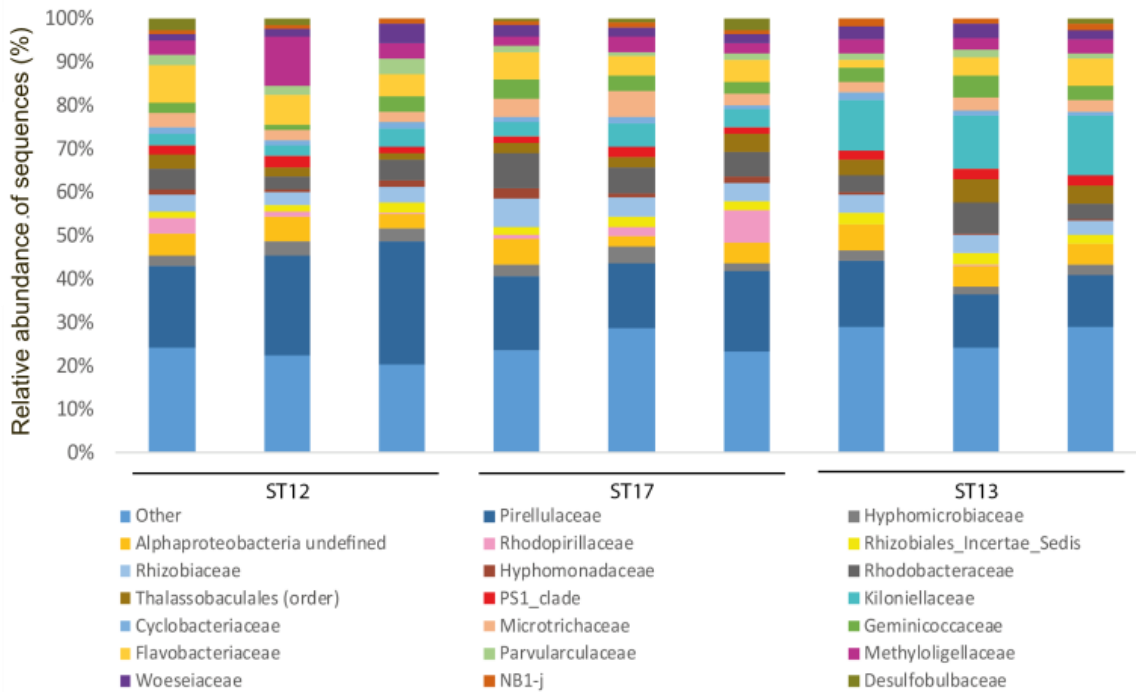


Figure 7. Multidimensional scaling ordination (MDS) of bacterial community composition. Bacteria communities associated with the CCA *Lithophyllum stictiforme* and *Mesophyllum sp.* sampled at different sites.



A



B

Figure 8. CCA bacteria taxonomy at the family level. Relative abundance of the 20 most abundant bacteria family associated with the two CCA morphotypes: **A.** *Lithophyllum stictiforme* and **B.** *Mesophyllum* sp.

	<i>L. stictiforme</i> %	<i>Mesophyllum</i> sp. %
BD1-7_clade	7	0
Gammaproteobacteria NA	2.5	0
Filomicrobium	2.9	0
Rhizobiaceae NA	2	0
Breoghania	2.3	0
Geminococcaceae NA	7.2	2.9
Pir4_lineage	4.3	9.3
Blastopirellula	2.1	2.4
Microtrichaceae NA	8.3	0
Ruegeria	1.9	0
Bythopirellula	0	4.3
Alphaproteobacteria NA	0	4.9
Thalassobaculales NA	0	3.2
PS1_clade NA	0	2.1
Kiloniellaceae NA	0	4.1
Methyloligellaceae NA	0	3.2
Woeseia	0	2.5

Figure 9. Most abundant CCA bacteria genera. Percentage contribution of the 10 most abundant bacteria genera of associated to *Lithophyllum stictiforme* and *Mesophyllum* sp.

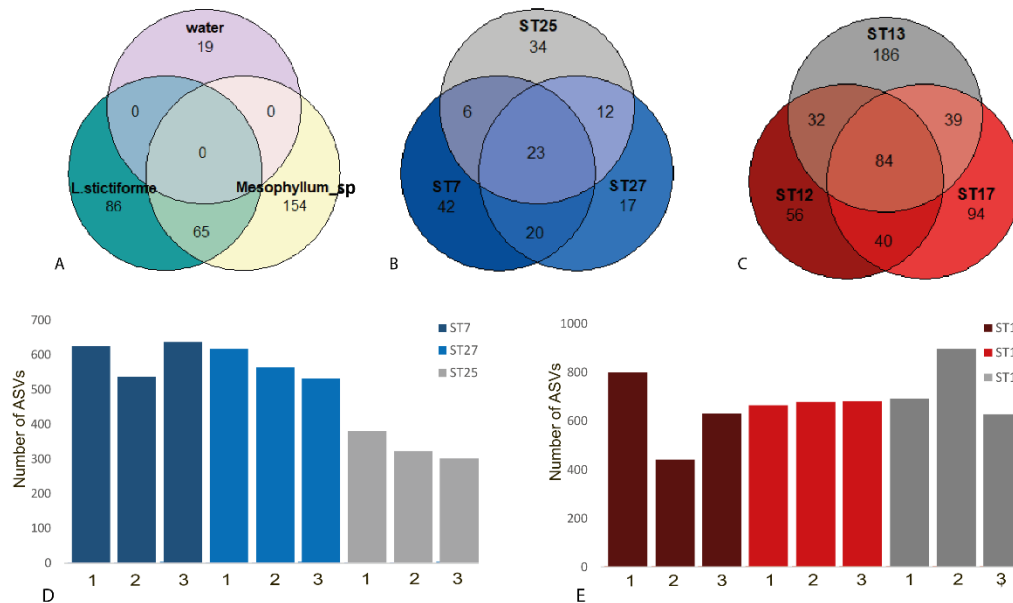
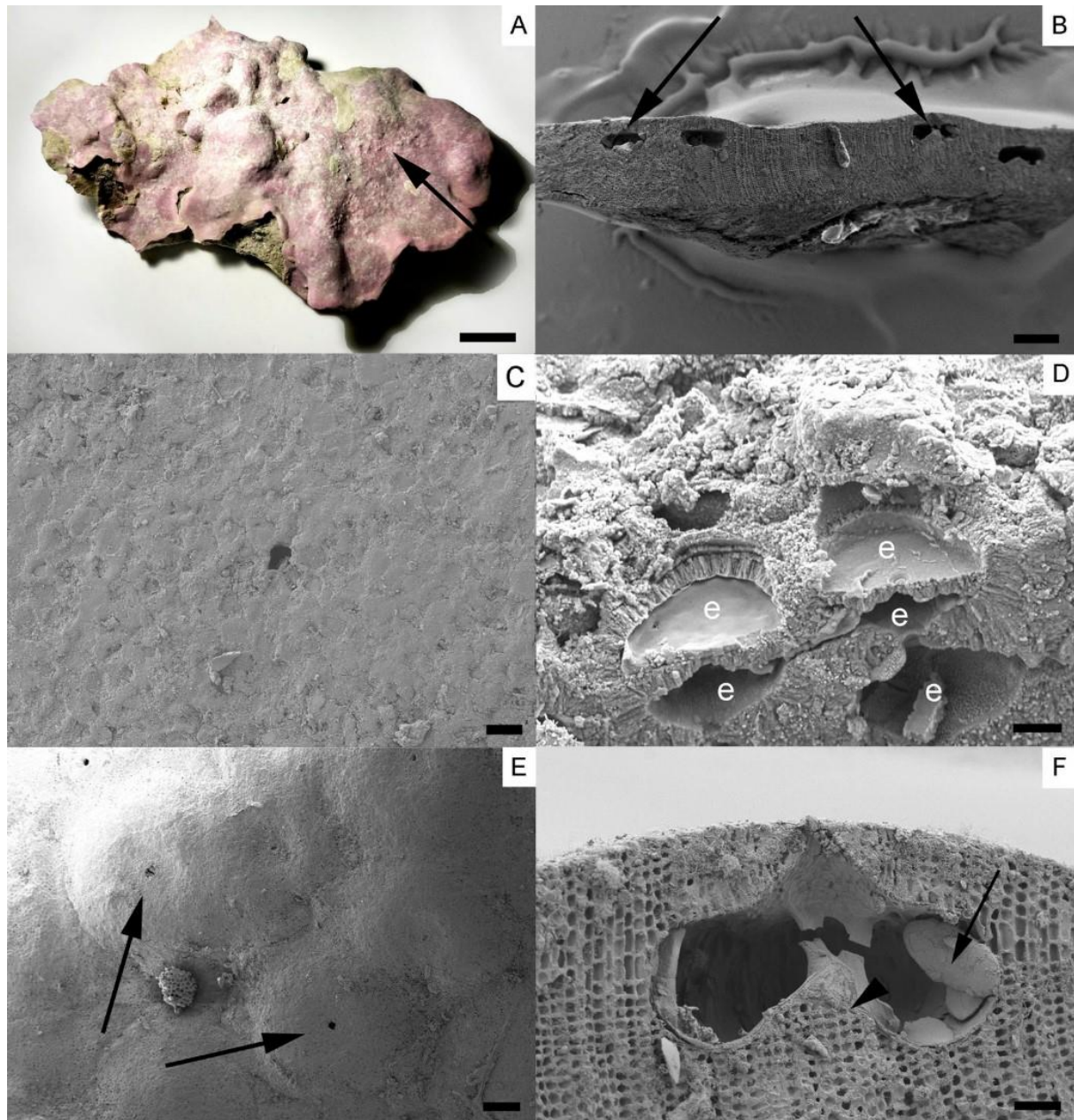


Figure 10. ASVs shared and ASVs number. **A.** ASVs shared between bacteria communities associated with water, *Lithophyllum stictiforme* and *Mesophyllum* sp. samples. **B.** ASVs shared between bacteria communities associated with *Lithophyllum stictiforme* at three sampling sites. **C.** ASVs shared between bacteria communities associated with *Mesophyllum* sp. at the three sampling sites. Number of ASVs characterizing the bacteria communities associated with all **D.** *Lithophyllum stictiforme* and **E.** *Mesophyllum* sp.

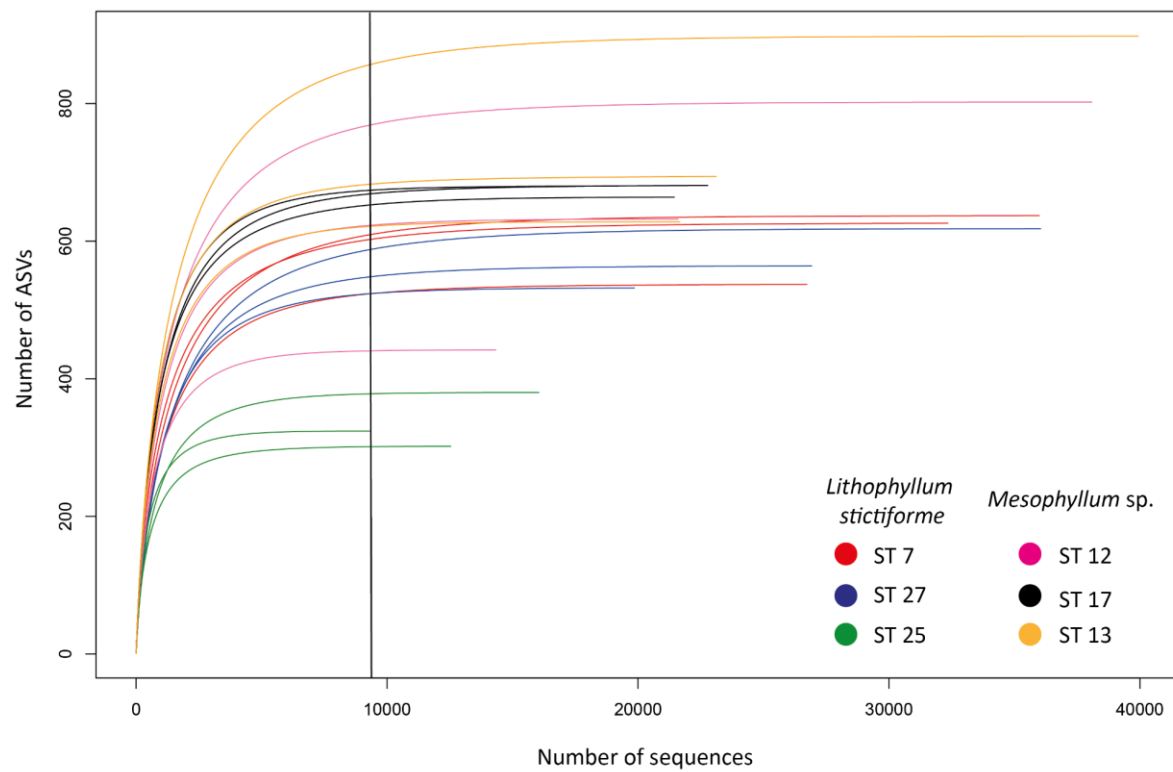
Table 1. Five most abundant shared and unique bacteria ASVs. ASVs are shown per category: shared between all CCA, all *Lithophyllum stictiforme* specimens and all *Mesophyllum* sp. specimens, and unique to all *Lithophyllum stictiforme* and all *Mesophyllum* sp. specimens.

	ASV	Order	Family	Species	Best match NCBI	Similarity	Origin	Reference
ASVs shared between the two CCA taxa bacteria communities	ASV 13	Rhizobiales	Hyphomicrobiaceae	Filomicrobium sp.	KF185466	100%	marine snow in North Adriatic Sea	Vojvoda et al., 2014
	ASV 14	Rhizobiales	Rhizobiaceae	NA	JQ236006	100%	biofilms from water purification system	Meron et al., 2012
	ASV 24	Rhizobiales	Hyphomicrobiaceae	Filomicrobium sp.	JX984050	100%	biofilms implicated in <i>M. edulis</i> settlement	Toupoint et al., 2012
	ASV 39	Rhodobacterales	Rhodobacteraceae	Ruegeria atlantica	MN704271	100%	sponges from the central coastal region of Vietnam	Dat et al., 2021
	ASV48	Microtrichales	Microtrichaceae	Sva0996_marine_group	JN113050	100%	marine sponge <i>Astroclera willeyana</i>	Yang & Li, 2012
ASVs unique of <i>L. stictiforme</i> bacteria communities	ASV 19	Pirellulales	Pirellulaceae	Pir4_lineage sp.	EU918001	98,32%	biofilm on artificial microbialites and natural stromatolites	Havemann et al., 2008
	ASV 22	Pirellulales	Pirellulaceae	Blastopirellula sp.	KT973101	100%	endolithic communities from intertidal outcrops	Couradeau et al., 2017
	ASV 30	Rhodobacterales	Rhodobacteraceae	Silicimonas sp.	MK175845	99,75%	coral <i>Astrangia poculata</i> microbiome	Goldsmith et al., 2019
	ASV 54	Thiohalorhabdales	Thiohalorhabdaceae	Granulosicoccus sp.	KY468648	96,49%	oil-polluted subtidal sediments North Spain coast	Acosta-González et al., 2013
	ASV 57	Pirellulales	Pirellulaceae	Pir4_lineage sp.	FJ652505	98,8%	sponge <i>Mycale laxissima</i>	Mohamed et al., 2010
ASVs unique of <i>Mesophyllum</i> sp. bacteria communities	ASV 7	Pirellulales	Pirellulaceae	Pir4_lineage	HM596354	98,56%	biofilm on condenser tube surfaces in a nuclear power plant	Choi et al., 2010
	ASV 34	Rhizobiales	Rhizobiaceae	NA	KT973129	97,76%	endolithic communities from marine intertidal outcrops	Couradeau et al., 2017
	ASV 41	Rhodobacterales	Rhodobacteraceae	Roseovarius sp.	KT973898	99%	endolithic communities from marine outcrops	Couradeau et al., 2018
	ASV 63	Pirellulales	Pirellulaceae	Blastopirellula sp.	EF215770	98,01%	surface biofilm in biofilm formation process in the West Pacific coast	Dang et al., 2008
	ASV 67	Pirellulales	Pirellulaceae	Pir4_lineage	FJ652505	98,08%	marine sponge <i>Mycale laxissima</i>	Mohamed et al., 2010
ASVs shared between <i>L. stictiforme</i> bacteria communities	ASV 13	Rhizobiales	Hyphomicrobiaceae	Filomicrobium sp.	KF185466	100%	marine snow in North Adriatic Sea	Vojvoda et al., 2014
	ASV 15	Rhizobiales	Stappiaceae	Breoghania sp.	HM177744	100%	CCA <i>Neogoniolithon fosliei</i>	Webster et al., 2011
	ASV 19	Pirellulales	Pirellulaceae	Pir4_lineage sp.	EU918001	98,32%	biofilm on artificial microbialites and natural stromatolites	Havemann et al., 2008
	ASV 22	Pirellulales	Pirellulaceae	Blastopirellula sp.	KT973101	100%	endolithic communities intertidal outcrops	Couradeau et al., 2017
	ASV 30	Rhodobacterales	Rhodobacteraceae	Silicimonas sp.	MK175845	99,75%	coral <i>Astrangia poculata</i> microbiome	Goldsmith et al., 2019
ASVs shared between <i>Mesophyllum</i> sp. bacteria communities	ASV 6	Pirellulales	Pirellulaceae	Bythopirellula sp.	JN596618	99,29%	tropical sponges, <i>Xestospongia muta</i> and <i>Xestospongia testudinaria</i>	Montalvo et al., 2011
	ASV 7	Pirellulales	Pirellulaceae	Pir4_lineage	HM596354	98,56%	biofilm on condenser tube surfaces in nuclear power plant	Choi et al., 2010
	ASV 13	Rhizobiales	Hyphomicrobiaceae	Filomicrobium sp.	KF185466	100%	marine snow in North Adriatic Sea	Vojvoda et al., 2014
	ASV 14	Rhizobiales	Rhizobiaceae	NA	JQ236006	100%	biofilms from water purification system	Meron et al., 2012
	ASV 23	Pirellulales	Pirellulaceae	Blastopirellula sp.	HM369093	99,26%	biofilms on surfaces of the kelp <i>Laminaria hyperborea</i>	Bengtsson et al., 2010

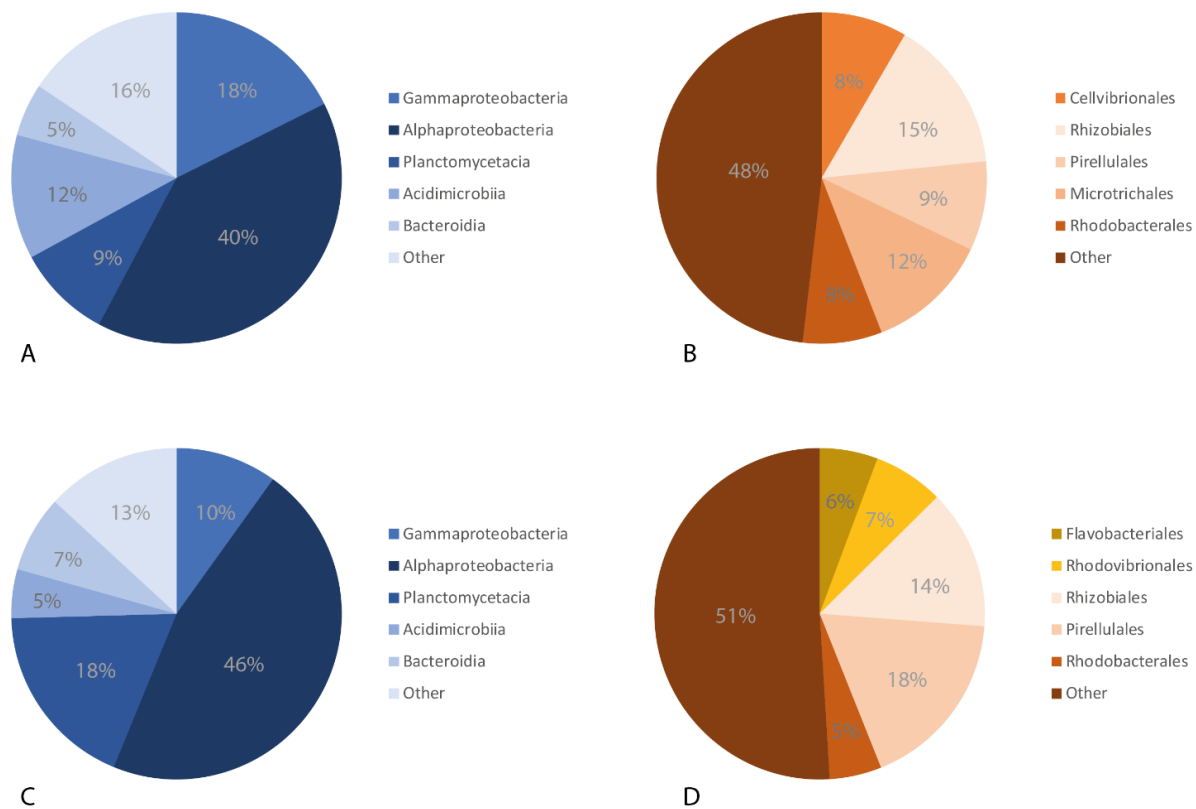
Supplementary figures



Supplementary Figure 1. Morphotype 1 - *Lithophyllum stictiforme* (Areschoug) Hauck samples from site ST25. A. Specimen with flat surface, free margins and uniporate conceptacles (arrow). Scale bar = 1 cm. **B.** Longitudinal section of the thallus with uniporate conceptacles (arrows). Scale bar = 300 μ m. **C.** Abraded surface of the thallus where the epithallial cells are not easily recognizable. Scale bar = 10 μ m. **D.** Filaments with 2-3 epithallial cells (e), the most superficial lacking the distal cell wall. Scale bar = 3 μ m. **E.** Uniporate conceptacles in surface (arrow). Scale bar = 100 μ m. **F.** Section through a tetrasporangial conceptacle with a prominent central columella (arrowhead) and laterally arranged tetrasporangia (arrow). Scale bar = 40 μ m.



Supplementary Figure 2. Rarefaction curves of all CCA bacterial community samples with rarefaction at 9310 sequences.



Supplementary Figure 3. Average relative abundance at class and order level of the five dominant bacteria ASVs associated with each CCA morphotype. **A.** Dominant bacteria classes and **B.** orders found in *Lithophyllum stictiforme* individuals; **C.** dominant bacteria classes and **D.** orders found in *Mesophyllum sp.* individuals.